An Excursion into Representative Volume Elements and Unit Cells

Shuguang Li and Elena Sitnikova

The University of Nottingham, Nottingham, United Kingdom

Abstract

The objective of this chapter is to provide a comprehensive and systematic account on the subject of representative volume elements (RVEs) and unit cells (UCs). To construct an RVE or UC, intuition has been often perceived sufficient to facilitate the analysis, but down to the details, approaches taken turn out to be rather mythological. It will be demonstrated in this chapter that there is absolutely no room for any myth on the subject if the basic concepts of mathematics and mechanics, *viz.* symmetry and free body diagrams, have been applied correctly and consistently. Only then, effective and reliable means of material characterisation based on the use of RVEs and UCs can be established, in particular, for composites where micro/meso-structures often dictate their behaviours. The logic employed defines the boundary of applicability of the methodology.

Keywords: Representative volume element (RVE); Unit cell (UC); Symmetry; Boundary conditions; Material characterisation; Micro/meso scales; Key degrees of freedom; 'Sanity checks'.

Table of Contents

1. Introduction

This chapter represents the very first attempt of putting together a systematic and comprehensive account on a specific subject of representative volume element (RVE) and unit cell (UC), which have found wide applications in modelling and characterisation of materials, in particular, composites. In the literature, they have been employed to facilitate specific analysis, often in a casual manner unfortunately. Readers are easily left with an impression that it is simply a routine step. However, once one has to put it in practice, all sorts of difficulties arise. The exercise is in fact full of pitfalls if one intends to adopt it as a serious means of material characterisation. There are so many seemingly trivial issues, but, without putting them right, one cannot even apply the analysis to an actually trivial problem!

It is not the objective of this chapter to provide a comprehensive literature review to list who did what and when. One of the reasons for not doing so is the fact that often one cannot find enough details in these publications in order to understand how they were done. Roughly, in nine out ten publications, one would not be able to reproduce the work due to the lack of information such as boundary conditions, load application and result processing. Amongst those cared to include an

account on boundary conditions, for instance, it was not uncommon to find statements, such as the boundary conditions were 'proposed to be', 'assumed to be', 'approximated as' or simply 'boundary conditions employed are', as if it was meant to be an account as loose as it was presented on one hand, or a well-known practice and hence does not require any justification, on the other hand. Where full details had been provided, few would stand scrutiny. Sometimes, simple anomalies could be identified straightaway, if the readers cared to observe. Simple testimonies can be the so-called 'sanity checks' as will be described fully later in the chapter. Another simple measure readers might exercise is to observe whether and how the analysis has involved shear stress state. Majority of the analyses using RVEs or UCs did not touch shear as if shear is either implied by the considerations made or unimportant. The truth is of course far from that. Shear is just as important as any other matrix dominated behaviour of composites. Even for a macroscopically isotropic material, prediction of shear stiffness is important to check if the isotropy has been preserved in the theoretical model as one of conditions for isotropy is $G = E / 2(1+v)$.

Multiscale modelling using RVEs and UCs can be a very effective tool for material characterisation, if it can be carried out systematically and consistently in a reliable manner. It has its own clearly defined boundary of applicability. The objective of this chapter is therefore to provide a comprehensive account on how it can be done systematically and consistently. The methodology can thus be established logically and hence reliably. Whilst following the logic behind each consideration, the myth over the subject can be dispelled, returning the subject a crystal clear account as it deserves.

2. Length Scales

The categorisation and characterisation of a material are always associated with a specific length scale. Historically, the length scale in engineering is macro, which was taken for granted in traditional studies, such as mechanics of materials, heat transfer, etc. Modern science and technology have allowed the human vision to be extended to substantially more refined scales. Materials can now be manipulated at meso (typically around millimetre), micro (from a few to tens of microns) and, nowadays, nano (from tens to hundreds of nanometers) scales. However, for practical applications of fibre reinforced composites, micro, meso and macro scales are common places. The discussion of this chapter will be confined within these scales. Even so, it crosses three scales. Without being overly restrictive in narrative, length scales will be referred to in a relative relationship as a lower length scale and an upper length scale. If the micro scale is considered as lower, the upper one could be meso as well as macro, while meso is the upper for micro but lower for macro. Meso scale is particularly relevant for textile composites, where fibre tows are interlocked into structures of regular patterns.

Multiscale nature is one of characteristics of composites. For material design and characterisation, it is often desirable to derive effective properties of a composite at an upper length scale from those of its constituents at a lower scale. The methodology established in present chapter is to offer a powerful means to facilitate this process.

3. Symmetry

The reflectional symmetries are undoubtedly the most familiar type to the readers. However, it will be very wrong to perceive that it is the only type of symmetry or the most important type of symmetry. In fact, there are three generic types of symmetries: translations, reflections and rotations [1]. One can of course cite more types, such as reflection about an axis, reflection about a point, etc. A careful examination will reveal that they are some combinations of these three generic ones. For instance, reflection about a point, or central reflection [2], is the combination of a reflection about a plane followed by a 180° rotation about the axis perpendicular to the plane of reflection.

A rotation of 360° is an identity transformation which is of little significance in the present discussion. A useful rotational symmetry about an axis is characterised by an angle which must be 360°/n, with n being an integer. It is often denoted as C^n. Rotational symmetries are just as important as reflectional symmetries. Reflectional symmetries can be absent from many micro/meso/macro structures where rotational symmetries are available. For example, laminates of arbitrary layup usually do not show any reflectional symmetry. However, they can be 180° rotationally symmetric about the axis perpendicular to the plane of the laminate [3].

Translational symmetry is often overlooked. However, in many ways, it is probably the most important type of symmetry in applications to material characterisation [4, 5, 6]. Without it, materials cannot be homogenised and unit cells cannot be established, as will be discussed in due course later.

4. Continuity and Free Body Diagrams

A physical problem is always defined in a domain over which some fields describe the contents of the problem. A physical field can be scalar, e.g. temperature, vectorial, e.g. displacement, or tensorial, e.g. stress. Continuity conditions are usually an essential requirement as a part of formulation of the physical problem. In a mechanical problem of deformation, for instance, continuity of displacement field is required by the deformation kinematics. In addition to the vectorial displacement field, this problem also involves tensor fields of stress, σ, and strain, ε. The continuity condition on stress is common place of confusion.

Stress field as a tensor does not have to be continuous. Equilibrium condition is not the continuity condition for stress. The continuity condition associated with stress is Newton's third law, as will be elaborated later in this section.

Free Body Diagram (FBD) is a very basic, yet essential, tool throughout this study. The essence of it is the continuity. Assume a body is separated into two free bodies by a plane perpendicular to the x axis at a coordinate x with the two surfaces created on each side of the two free bodies denoted as x^- and x^+, respectively. The continuity of the displacement field requires

$$\left\{\begin{matrix} u \\ v \\ w \end{matrix}\right\}\Bigg|_{x^+} = \left\{\begin{matrix} u \\ v \\ w \end{matrix}\right\}\Bigg|_{x^-} . \tag{1}$$

Without such continuity condition as expressed through the vehicle of FBD, deformation of the body would result in slits or overlaps in the body, which violates the deformation kinematics.

The continuity condition associated with the stress is presented in terms of traction. On a plane with an outward normal, $\{n\}$, traction is defined as $\{S\}=[\sigma]\{n\}$, in general. On the plane perpendicular to the x axis,

$$\{n\} = \left\{\begin{matrix} 1 \\ 0 \\ 0 \end{matrix}\right\} \quad \text{thus} \quad \{S\} = \left\{\begin{matrix} \sigma_x \\ \tau_{xy} \\ \tau_{xz} \end{matrix}\right\}. \tag{2}$$

At x^- and x^+, i.e. the two surfaces created in the free bodies as mentioned above, the outward normals are

$$\{n\}\big|_{x^-} = \left\{\begin{matrix} 1 \\ 0 \\ 0 \end{matrix}\right\} \quad \text{and} \quad \{n\}\big|_{x^+} = \left\{\begin{matrix} -1 \\ 0 \\ 0 \end{matrix}\right\}, \text{ respectively.} \tag{3}$$

The traction on them are therefore

$$\{S\}\big|_{x^-} = \left\{\begin{matrix} \sigma_x \\ \tau_{xy} \\ \tau_{xz} \end{matrix}\right\} \quad \text{and} \quad \{S\}\big|_{x^+} = -\left\{\begin{matrix} \sigma_x \\ \tau_{xy} \\ \tau_{xz} \end{matrix}\right\}, \text{ respectively.} \tag{4}$$

$\{S\}\big|_{x^-}$ and $\{S\}\big|_{x^+}$ are action and reaction for each other. Newton's third law requires

$$\{S\}\big|_{x^-} = -\{S\}\big|_{x^+} \qquad \text{i.e.} \qquad \begin{Bmatrix} \sigma_x \\ \tau_{xy} \\ \tau_{xz} \end{Bmatrix}\Bigg|_{x^-} = \begin{Bmatrix} \sigma_x \\ \tau_{xy} \\ \tau_{xz} \end{Bmatrix}\Bigg|_{x^+} . \qquad (5)$$

It should be noted clearly here that the stress components shown above form the tractions as vectors on the exposed surfaces of the free bodies. Continuity of them as in (5) is required by Newton's third law, not equilibrium, which is governed by Newton's first law. Readers are reminded that the action and reaction act on different bodies and hence are not in equilibrium. It is obvious that the continuity associated with stress is not for the stress as a whole, but for those components exposed on the surface concerned to form the traction. Other stress components are irrelevant, as Newton's third law does not have any bearing on them.

Equations (1) and (5) are the continuity conditions as obtained from the FBD.

5. Symmetry Conditions

A transformation means a change in shape or position of an object. If the shape or position remains unchanged after a transformation, the transformation is a symmetry transformation. It is often referred to simply as a symmetry.

Symmetry in the context of the present discussion is a geometric, as well as a physical property. Its applications in physical disciplines require a little extension of the concept to the physical fields under consideration. Physical fields usually have their senses. If a field is multiplied by -1, it is converted to its opposite sense. The involvement of the sense enriches the concept of symmetry, but also causes confusion as a by-product. Under a symmetry transformation in accordance with the geometric symmetry, a physical field could be symmetric, if the field keeps its sense under the symmetry transformation, or antisymmetric if the field changes to its opposite sense under the symmetry transformation.

When symmetries are made use of in a physical problem, they will result in some conditions which are implied by the symmetry. To make these conditions explicit, free body diagrams will have to be resorted to. Once these conditions are combined with the continuity conditions, they offer the so-called symmetry conditions. This will be illustrated for each of the three symmetries as follows. Without losing generality, a mechanical problem of deformation will be considered, which involves a vector field of displacement, u, and a tensor field of stress, σ.

5.1 Translational symmetry

Assume the translation is in the x direction by a distance of Δx. An arbitrary segment of length Δx in the domain for the physical problem between x_0 and $x_0+\Delta x$ will be selected to produce the free body diagram. The presence of translational symmetry for the geometry and the physical

properties does not necessary imply that all physical fields involved possess the same symmetry. In fact, even with perfectly uniform stress distribution, where the translational symmetry for stress field is obvious, the associated displacement field does not possess translational symmetry. Consider a uniform deformation at the upper length scale in a 1D case as an example. The displacement field, u, can be defined as a linear function of coordinate x as follows:

$$u(x) = \varepsilon x + u_R \ , \tag{6}$$

where ε and u_R are constants with the former being the effective strain and latter the displacement at a reference point.

As shown in Figure 1, such displacement field is obviously not periodic and there is no translational symmetry. At the same time, stress and strain fields associated with it are both periodic and hence translationally symmetric, because they are both uniform.
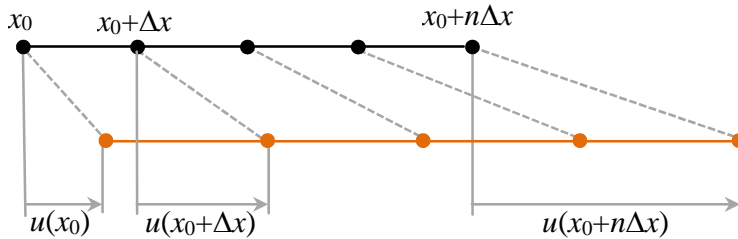
Figure 1 Linear 1D displacement field corresponding to a uniform strain field

This has often been a source of confusion. In order to apply the translational symmetry to displacement, one has to resort to the relative displacement field instead. Select any point R at x_R as a reference within segment $[x_0, x_0+\Delta x]$. Assume the point of interest is P at x within the segment. The displacement of P relative to that of R is given as

$$\left. \begin{Bmatrix} u \\ v \\ w \end{Bmatrix} \right|_{x} - \left. \begin{Bmatrix} u \\ v \\ w \end{Bmatrix} \right|_{x_R} \ , \tag{7}$$

and that in the next segment is

$$\left. \begin{Bmatrix} u \\ v \\ w \end{Bmatrix} \right|_{x+\Delta x} - \left. \begin{Bmatrix} u \\ v \\ w \end{Bmatrix} \right|_{x_R+\Delta x} \ , \tag{8}$$

and so on and so forth. Relative displacements in both segments referred to above are identical. A relative displacement field can thus be defined segment by segment. There is a translational symmetry, or periodicity, in the relative displacement field as defined, as shown (red) in Figure 2. It is worth noting that the relative displacement field is not continuous. However, this should not be any cause for concern as long as the displacement field associated with it is continuous, as it is indeed the case, given its linear appearance (green in Figure 2).
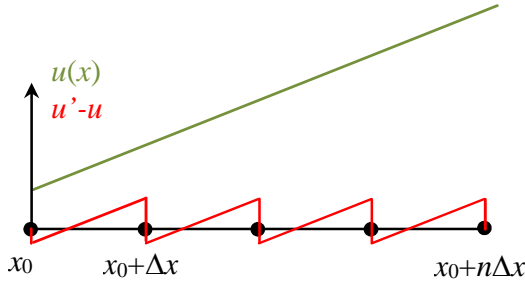

Figure 2 Schematic illustration of the relative displacement field (zigzag) in contrast with the displacement field (straight line)

When x is placed on the boundary of the segment, the symmetry transformation gives

$$
\left\{ \begin{array}{c} u \\ v \\ w \end{array} \right\}\Bigg|_{x_0^+} - \left\{ \begin{array}{c} u \\ v \\ w \end{array} \right\}\Bigg|_{x_R} = \left\{ \begin{array}{c} u \\ v \\ w \end{array} \right\}\Bigg|_{x_0^+ + \Delta x} - \left\{ \begin{array}{c} u \\ v \\ w \end{array} \right\}\Bigg|_{x_R + \Delta x} , \tag{9}
$$

$$
\left\{ \begin{array}{c} u \\ v \\ w \end{array} \right\}\Bigg|_{x_0^-} - \left\{ \begin{array}{c} u \\ v \\ w \end{array} \right\}\Bigg|_{x_R} = \left\{ \begin{array}{c} u \\ v \\ w \end{array} \right\}\Bigg|_{x_0^- + \Delta x} - \left\{ \begin{array}{c} u \\ v \\ w \end{array} \right\}\Bigg|_{x_R + \Delta x} .
$$

The displacement (not the relative displacement) field must be continuous across the boundaries of segments as established from the consideration of FBD in the previous section. Thus

$$
\left\{ \begin{array}{c} u \\ v \\ w \end{array} \right\}\Bigg|_{x_0^-} = \left\{ \begin{array}{c} u \\ v \\ w \end{array} \right\}\Bigg|_{x_0^+} \quad \text{and} \quad \left\{ \begin{array}{c} u \\ v \\ w \end{array} \right\}\Bigg|_{x_0^- + \Delta x} = \left\{ \begin{array}{c} u \\ v \\ w \end{array} \right\}\Bigg|_{x_0^+ + \Delta x} . \tag{10}
$$

Therefore, (9) can be re-written as follows

$$\left\{ \begin{array}{c} u \\ v \\ w \end{array} \right\}\Bigg|_{x_0^+} - \left\{ \begin{array}{c} u \\ v \\ w \end{array} \right\}\Bigg|_{x_R} = \left\{ \begin{array}{c} u \\ v \\ w \end{array} \right\}\Bigg|_{x_0^-+\Delta x} - \left\{ \begin{array}{c} u \\ v \\ w \end{array} \right\}\Bigg|_{x_R+\Delta x}. \tag{11}$$

Eliminating those at $(\ )|_{x_0^-}$ and $(\ )|_{x^++\Delta x}$ which are not part of the segment concerned, one obtains the translational symmetry condition for the displacement as

$$\left\{ \begin{array}{c} u \\ v \\ w \end{array} \right\}\Bigg|_{x_0^-+\Delta x} - \left\{ \begin{array}{c} u \\ v \\ w \end{array} \right\}\Bigg|_{x_0^+} = \left\{ \begin{array}{c} u \\ v \\ w \end{array} \right\}\Bigg|_{x_R+\Delta x} - \left\{ \begin{array}{c} u \\ v \\ w \end{array} \right\}\Bigg|_{x_R}. \tag{12}$$

Similarly, through the same argument, the translational symmetry condition for the traction can be obtained as

$$\left\{ \begin{array}{c} \sigma_x \\ \tau_{xy} \\ \tau_{xz} \end{array} \right\}\Bigg|_{x_0^+} = \left\{ \begin{array}{c} \sigma_x \\ \tau_{xy} \\ \tau_{xz} \end{array} \right\}\Bigg|_{x_0^-+\Delta x}. \tag{13}$$

These are conditions for displacement and stress components on the two sides of the segment that have to be satisfied. If the segment is to be analysed as a UC, these will be the boundary conditions for the UC in this one-dimensional case. The relative displacements between segments at fixed points within respective segment as appearing on the right hand side of (12) can be easily associated with the average strains. This will be discussed in details in Section 9.

For practicality, only symmetric transformations of physical fields will be considered for translational symmetries. Antisymmetry is not dealt with here.

5.2 Reflectional symmetry

Assume the reflection is about a plane perpendicular to the x axis located at x_0. Split the domain by the plane in the sense of free body diagram as shown in Figure 3(a). The continuity of the displacements and traction requires

$$\left\{ \begin{array}{c} u \\ v \\ w \end{array} \right\}\Bigg|_{x_0^+} = \left\{ \begin{array}{c} u \\ v \\ w \end{array} \right\}\Bigg|_{x_0^-} \quad \text{and} \quad \left\{ \begin{array}{c} \sigma_x \\ \tau_{xy} \\ \tau_{xz} \end{array} \right\}\Bigg|_{x_0^+} = \left\{ \begin{array}{c} \sigma_x \\ \tau_{xy} \\ \tau_{xz} \end{array} \right\}\Bigg|_{x_0^-}. \tag{14}$$

If the physical fields under consideration are symmetric as shown in Figure 3(b), the symmetry transformation requires
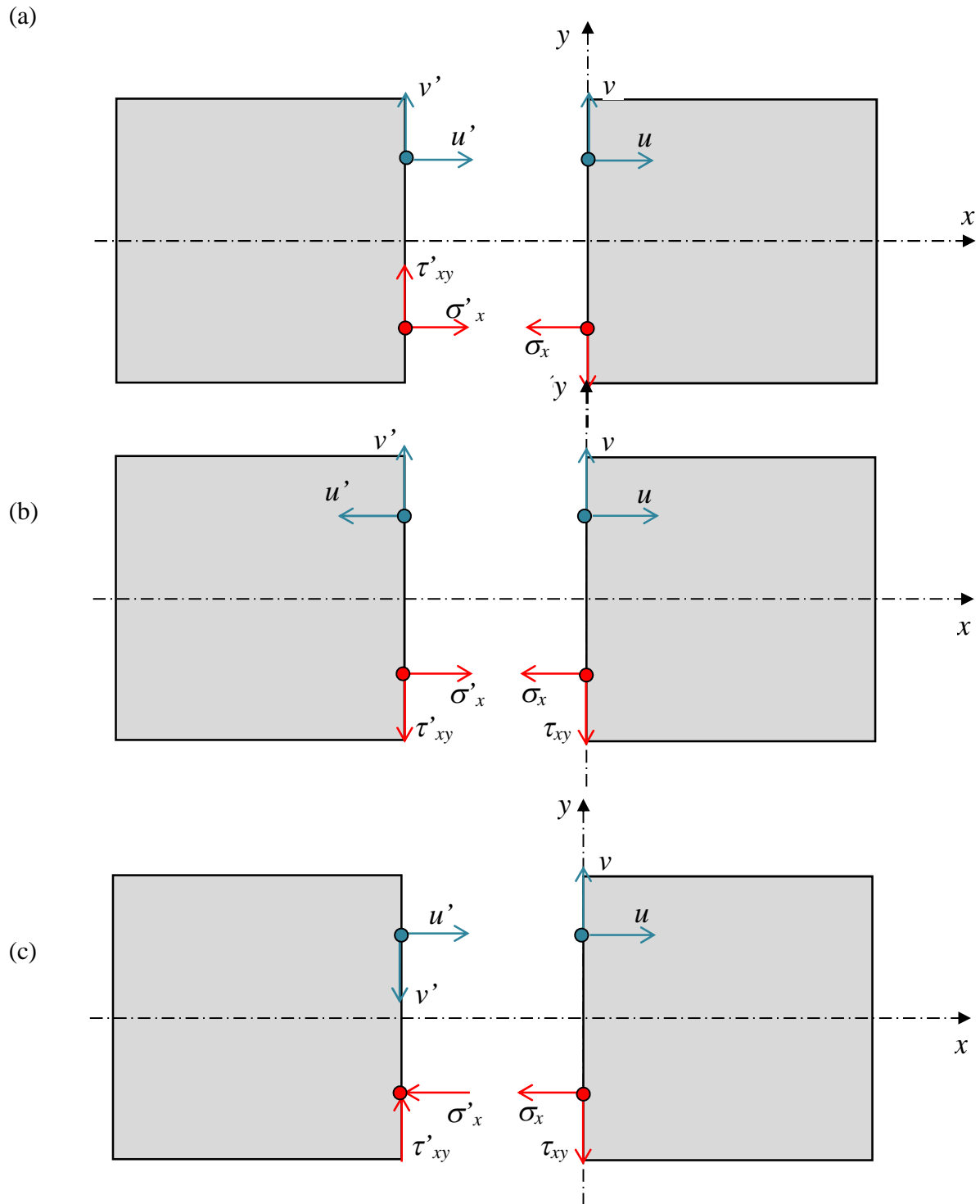
(a)

(b)

(c)

Figure 3 (a) Free body diagram to show the continuity of displacements and stresses, and (b) symmetric and (c) antisymmetric reflectional symmetry of the displacements and stresses

$$\left\{\begin{matrix} u \\ v \\ w \end{matrix}\right\}\Bigg|_{x_0^+} = \left\{\begin{matrix} -u \\ v \\ w \end{matrix}\right\}\Bigg|_{x_0^-} \quad \text{and} \quad \left\{\begin{matrix} \sigma_x \\ \tau_{xy} \\ \tau_{xz} \end{matrix}\right\}\Bigg|_{x_0^+} = \left\{\begin{matrix} \sigma_x \\ -\tau_{xy} \\ -\tau_{xz} \end{matrix}\right\}\Bigg|_{x_0^-} . \tag{15}$$

If the physical fields under consideration are antisymmetric, the symmetry transformation requires

$$\left\{\begin{matrix} u \\ v \\ w \end{matrix}\right\}\Bigg|_{x_0^+} = \left\{\begin{matrix} u \\ -v \\ -w \end{matrix}\right\}\Bigg|_{x_0^-} \quad \text{and} \quad \left\{\begin{matrix} \sigma_x \\ \tau_{xy} \\ \tau_{xz} \end{matrix}\right\}\Bigg|_{x_0^+} = \left\{\begin{matrix} -\sigma_x \\ \tau_{xy} \\ \tau_{xz} \end{matrix}\right\}\Bigg|_{x_0^-} . \tag{16}$$

In each case, symmetric or antisymmetric, one can eliminate those at $\left(\ \right)\big|_{x^-}$ by considering (14) and (15), or (14) and (16) as a set of simultaneous equations. For symmetric case, one obtains

$$u\big|_{x_0^+} = 0 \quad \text{and} \quad \tau_{xy}\big|_{x_0^+} = \tau_{xz}\big|_{x_0^+} = 0, \tag{17}$$

for antisymmetric case, one obtains

$$v\big|_{x_0^+} = w\big|_{x_0^+} = 0 \quad \text{and} \quad \sigma_x\big|_{x_0^+} = 0, \tag{18}$$

which are conditions for displacements and stresses on the symmetry plane that have to be satisfied for symmetric and antisymmetric cases, respectively.

5.3 180° rotational symmetry

Like reflectional symmetries, rotational symmetries can be either symmetric or antisymmetric depending on the loading conditions. The conditions implied by the symmetry can again be derived from two considerations, continuity and symmetry. Illustrated in Figure 4 are the free body diagram and the symmetric symmetry transformation of displacements and the tractions in the surface, whilst the antisymmetric counterparts to Figure 4(b) and (c) can be produced by the readers easily and hence are not included here. In Figure 4, the coordinate system is deliberately chosen to be different from that in Figure 3. As will be seen later, materials having a reflectional symmetry about a plane perpendicular to the *x*-axis are categorised in exactly the same group as those having a rotational symmetry about the *x*-axis.

In this study, rotational symmetries will be limited to 180° rotations, i.e. C^2. An example involving other angles in the context of polar coordinate applications can be found in [7] although it will not be covered in this chapter.

(a)
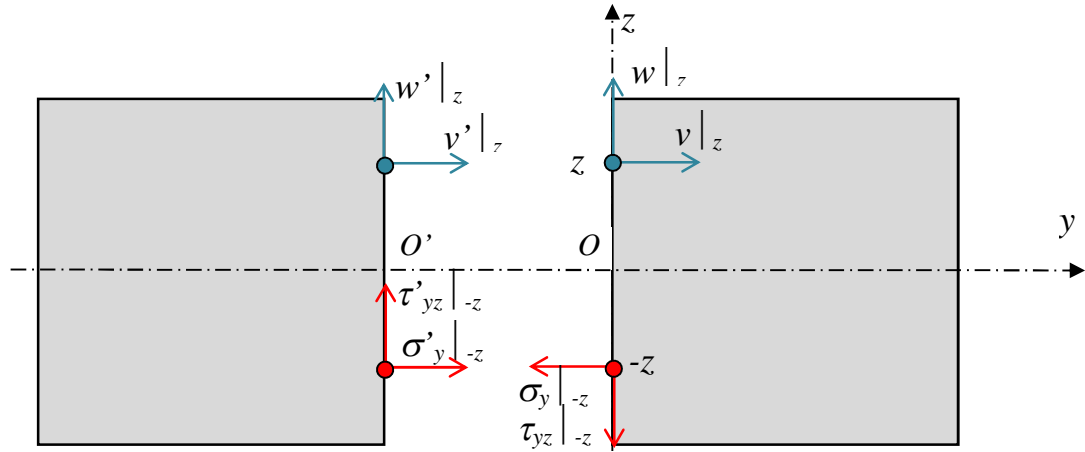
(b)
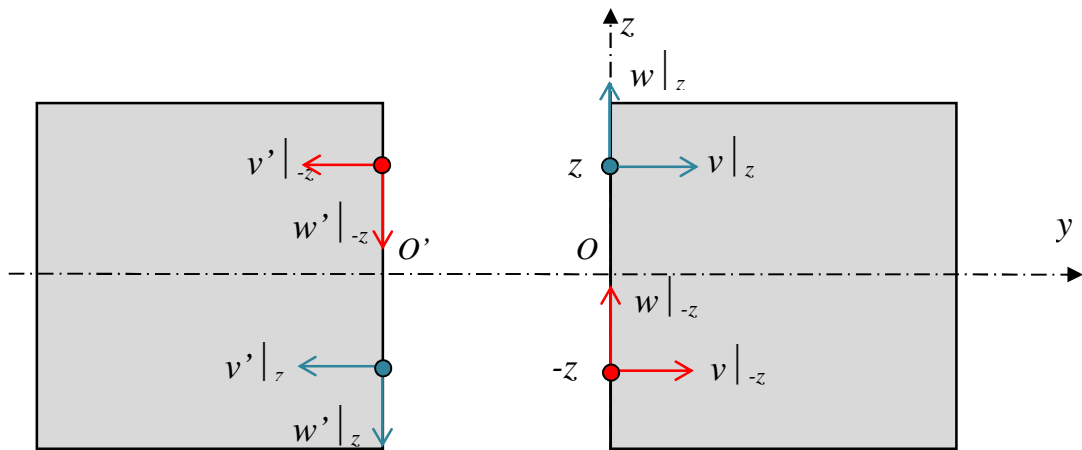
(c)

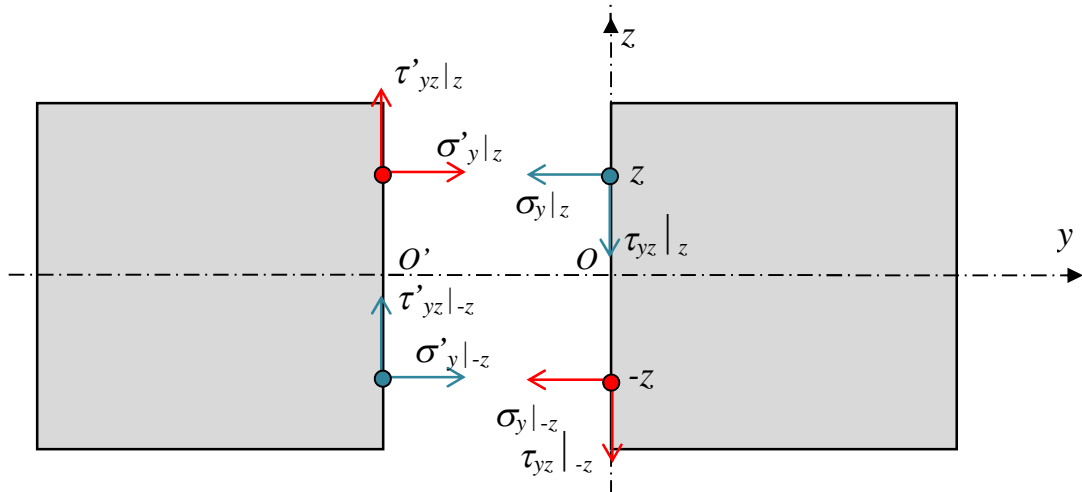Figure 4(a) Free body diagram to show the continuity of displacements and stresses, (b) symmetric rotational symmetry of the displacements and (c) symmetric rotational symmetry of the stresses

Assume the 180° rotational symmetry is about the *x* axis. The way to split the domain into two halves in the sense of free body diagram is no longer unique. The partitioning surface does not even have to be a plane. The conditions for it are that it passes the axis of rotation and is rotationally symmetric about the same axis. For argument's sake, it is chosen as the plane perpendicular to the *y* axis. The continuity of the displacement and stress fields requires

$$\left\{\begin{matrix} u \\ v \\ w \end{matrix}\right\}\Bigg|_{y=0^+,z} = \left\{\begin{matrix} u \\ v \\ w \end{matrix}\right\}\Bigg|_{y=0^-,z} , \tag{19}$$

$$\left\{\begin{matrix} \tau_{yx} \\ \sigma_y \\ \tau_{yz} \end{matrix}\right\}\Bigg|_{y=0^+,z} = \left\{\begin{matrix} \tau_{yx} \\ \sigma_y \\ \tau_{yz} \end{matrix}\right\}\Bigg|_{y=0^-,z} . \tag{20}$$

If the physical fields under consideration are symmetric, the symmetry transformation requires

$$\left\{\begin{matrix} u \\ v \\ w \end{matrix}\right\}\Bigg|_{y=0^+,z} = \left\{\begin{matrix} u \\ -v \\ -w \end{matrix}\right\}\Bigg|_{y=0^-,-z} , \tag{21}$$

$$\left\{\begin{matrix} \tau_{yx} \\ \sigma_y \\ \tau_{yz} \end{matrix}\right\}\Bigg|_{y=0^+,z} = \left\{\begin{matrix} -\tau_{yx} \\ \sigma_y \\ -\tau_{yz} \end{matrix}\right\}\Bigg|_{y=0^-,-z} . \tag{22}$$

If the physical fields under consideration are antisymmetric, the symmetry transformation requires

$$\left\{\begin{matrix} u \\ v \\ w \end{matrix}\right\}\Bigg|_{y=0^+,z} = \left\{\begin{matrix} -u \\ v \\ w \end{matrix}\right\}\Bigg|_{y=0^-,-z} , \tag{23}$$

$$\left\{\begin{matrix} \tau_{yx} \\ \sigma_y \\ \tau_{yz} \end{matrix}\right\}\Bigg|_{y=0^+,z} = \left\{\begin{matrix} \tau_{yx} \\ -\sigma_y \\ \tau_{yz} \end{matrix}\right\}\Bigg|_{y=0^-,-z} . \tag{24}$$

After eliminating those on $\left.(\ \ )\right|_{y^-}$ for symmetric or antisymmetric cases respectively, the conditions are

$$
\left.\begin{Bmatrix} u \\ v \\ w \end{Bmatrix}\right|_{y=0^+,z} = \left.\begin{Bmatrix} u \\ -v \\ -w \end{Bmatrix}\right|_{y=0^+,-z} \quad \text{and} \quad \left.\begin{Bmatrix} \tau_{yx} \\ \sigma_y \\ \tau_{yz} \end{Bmatrix}\right|_{y=0^+,z} = \left.\begin{Bmatrix} -\tau_{yx} \\ \sigma_y \\ -\tau_{yz} \end{Bmatrix}\right|_{y=0^+,-z} \tag{25}
$$

for the symmetric case, and

$$
\left.\begin{Bmatrix} u \\ v \\ w \end{Bmatrix}\right|_{y=0^+,z} = \left.\begin{Bmatrix} -u \\ v \\ w \end{Bmatrix}\right|_{y=0^+,-z} \quad \text{and} \quad \left.\begin{Bmatrix} \tau_{yx} \\ \sigma_y \\ \tau_{yz} \end{Bmatrix}\right|_{y=0^+,z} = \left.\begin{Bmatrix} \tau_{yx} \\ -\sigma_y \\ \tau_{yz} \end{Bmatrix}\right|_{y=0^+,-z} \tag{26}
$$

for the antisymmetric case. These are conditions of displacement and stress field to be satisfied on the *y*-plane selected as the partition plane, for symmetric and antisymmetric cases respectively. They will be the boundary conditions for the half domain to be analysed on the $y \geq 0$ side.

It can be seen above that the translational symmetry is the only one which can reduce the domain from infinite to finite. The price to pay is to accept and to deal with the concept of relative displacement field.

Either reflectional or rotational symmetry can only reduce an infinite domain to semi-infinite, which is still infinite in extent. In this respect, reflectional and rotational symmetries have often been subjected to abuses. In order to reduce an infinite domain using reflectional or rotational symmetries alone, there have been attempts, as have often been observed in the literature, to use the symmetry twice with the partition planes placed adjacent to each other in parallel by a distance equal to the distance for the existing translational symmetry, without using the translational symmetry. This was done sometimes explicitly, where error can be easily tracked, and sometimes implicitly whilst giving no justification whatsoever. In fact, users of the latter group soon found that it was not quite right and they had to artificially relax the constraints imposed by the symmetry somehow to allow certain patterns of deformation prohibited by the symmetry consideration in place. Any relaxation therefore conflicts the symmetry by definition. It is not difficult to dismiss such an approach. The first use of a reflectional or rotational symmetry has reduced the infinite domain to a semi-infinite one. The semi-infinite domain does no longer possess the same symmetry anymore, as is schematically illustrated in Figure 5(a). A typical example of such confusion can be found in the so-called equivalent coordinate systems (ECS) [8].

14

On the other hand, via the use of the translational symmetry an infinite domain can be reduced to a finite extent, as shown in Figure 5(b). In fact, out of the three generic types of symmetries, only the translational ones have the capability of reducing an infinite domain to a finite one.

(a)

Infinite

Symmetry
conditions

Infinite

Reflectional symmetry is no longer available

(b)

Infinite

Periodic
boundary
conditions

Periodic
boundary
conditions

Infinite

Translational symmetry / Periodicity — always applies
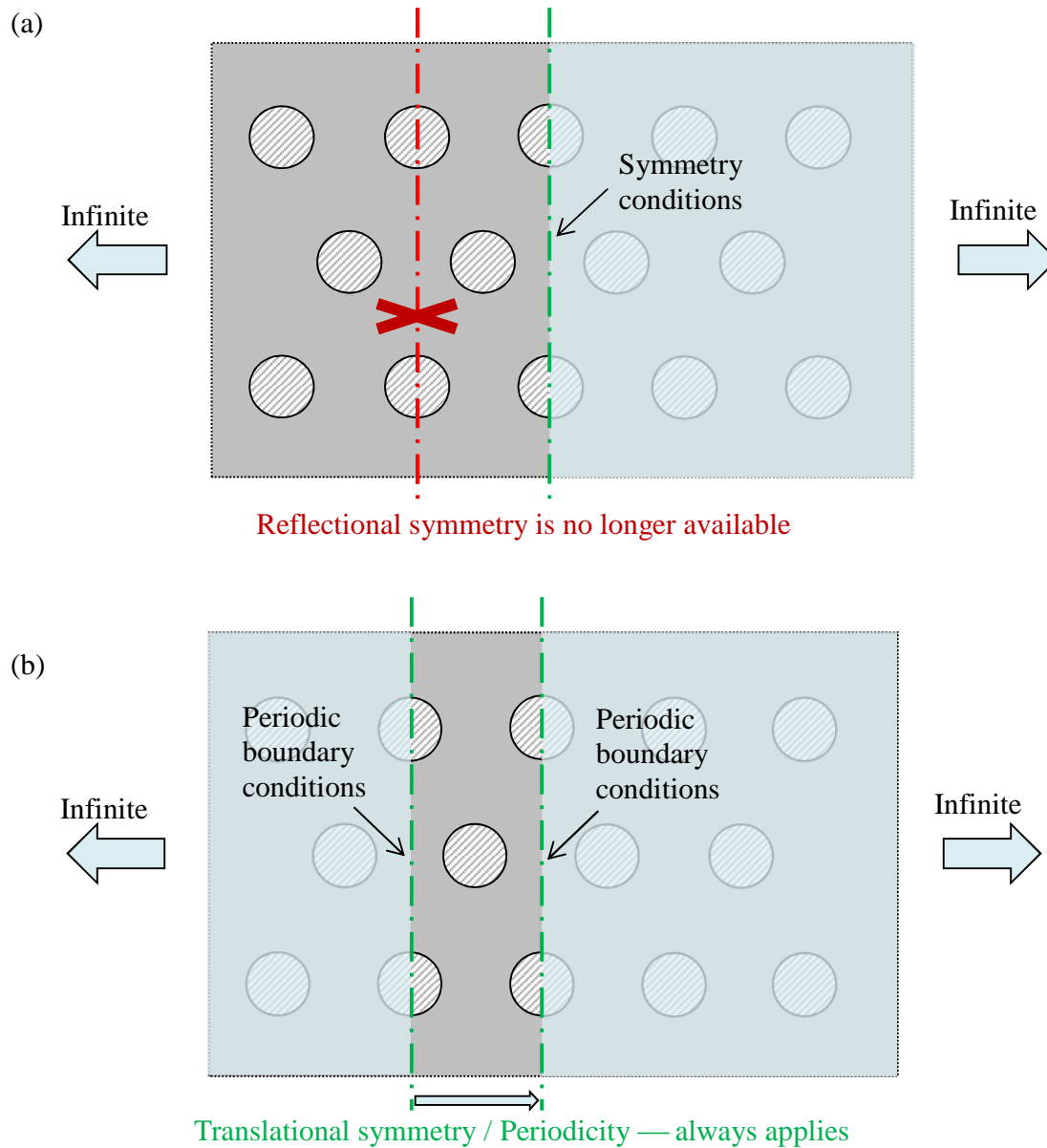
Figure 5 (a) Applicability of reflectional symmetry and (b) the use of translational symmetry to reduce from an infinite domain to finite

Another factor associated with reflectional and rotational symmetries is that the sense of symmetry transformation can be symmetric as well as antisymmetric. This causes complications as well as confusions from time to time. When using them to formulate unit cells, sufficient care must be exercised to avoid mistakes.

16

To summarise the discussion on the conditions resulting from symmetry considerations to be used as boundary conditions for the physical problem concerned in a domain of reduced size, it has been clearly demonstrated above that it can be done systematically. There are only two considerations, continuity as reflected in the use of a free body diagram and the symmetry transformation on physical fields concerned. Typical error in the application of symmetries often resulted from plausible extension of intuition without due respect to scientific rigor. Whilst rigor could be tedious from time to time, intuition has its own limit. Unfounded extension has always been the recipe for errors.

The boundary conditions given in terms of stress components above are called traction boundary conditions in the theory of elasticity. If the subsequent analyses are carried out using finite elements (FE), as is the case for most applications, another important point should be made. The theory of FE is formulated on a variational principle, typically the minimum total potential principle, which is displacement-based. Variational calculus states that the stationary value condition of the energy functional is equivalent to the satisfaction of the Euler's equation and the natural boundary condition, together [9]. For an elasticity problem, the Euler's equation reproduces the equilibrium equation and the natural boundary condition is the traction boundary condition. As a result, in practical FE analyses, traction boundary conditions as obtained from symmetry considerations should not be imposed as they have been satisfied, usually, approximately, when the stiffness equation from the FE analysis are satisfied, again approximately usually, because the satisfaction of the stiffness equation is equivalent to the satisfaction of the stationary value condition which includes the satisfaction of the natural boundary. It should also be pointed out that the approximation in the natural boundary condition should not be improved by imposing the traction boundary conditions upfront as displacement boundary conditions. Although this could have the natural boundary condition satisfied exactly, it is always at the cost of the worst overall approximation, as doing so prevents the energy functional to be minimised. According to the error theory of finite elements, the lower the value of the energy functional, the better the overall approximation. In reality, imposition of traction boundary conditions is very hard to implement. One could make enormous efforts only to spoil the accuracy of the results, without a clear concept of natural boundary conditions. An illustration can be found in [10].

6. Material Categorisation

Any serious application of a material requires relevant properties of the material to become known. The process of obtaining such properties is often referred to as material characterisation. As material characterisation is such an important procedure, there is a danger to jump to it blindly. It is therefore wise to put up a warning sign here by splitting the process into two steps, material categorisation and material characterisation. The former is more of qualitative nature while the latter is quantitative.

Categorisation is to put the material concerned into an appropriate category, in particular, in terms of its heterogeneity and anisotropy. The simplest descriptors, such as homogeneity, isotropy and linearity, are usually assumed in introductory courses, such as, strength of materials, theory of elasticity, mechanics of composites, etc.. They are therefore often been taken for granted, as in this case there is nothing left for categorisation. However, when heterogeneous and anisotropic materials are involved, categorisation is no longer a step that can be skipped. The extent of heterogeneity, degree of anisotropy and severity of nonlinearity are always significant considerations in the material selection phase of any serious engineering design.

In material categorisation, homogeneity is undoubtedly the most important descriptor to examine, although it is often taken for granted. Without it, the behaviour of a material will vary from point to point. Whilst there are materials, natural or engineered, such as bones and functionally graded materials, showing noticeable variation of material properties in space, a plane or a direction, their characterisation is inevitably a rather specialised study and therefore will be beyond the scope of this chapter. The materials concerned in the present discussion are assumed to be homogeneous at least at one length scale and the material is expected to be used in engineering within this length scale or above. Heterogeneity is present at lower length scales. The task of so-called micromechanics is to homogenise the heterogeneity at a lower length scale so that the material can be treated as homogeneous for engineering applications at the upper length scale. In order to achieve such homogenisation, one can find the concept of RVEs for materials of random structures and UCs for materials of regular structures at a lower length scale useful means. The underlying type of symmetry to facilitate this categorisation is translation. A material is effectively homogeneous if it possesses translational symmetries in three non-coplanar directions, either in a statistical sense or a rigorous geometric sense, where the minimum distances of these translations determine the characteristic dimensions of the RVE or UC.

Having achieved the homogeneity, the next logical step is to categorise the material's anisotropy, where one will find reflectional and rotational symmetries to be of great assistance, either in a statistical sense or a rigorous geometric sense.

With a reflectional symmetry about one plane, the material can be categorised as monoclinic. The plane is the principal plane of the monoclinic material. With this, the number of material constant required to characterise its behaviour drops from 21 to 13 for elasticity and from 6 to 4 for thermal expansion and for a diffusion problem, such as heat/electric conduction and permeability of fluid in porous materials. The existence of a further reflectional symmetry about a plane perpendicular to the existing principal plane reduces the material to orthotropy. The presence of two perpendicular principal planes implies that the third plane perpendicular to the two principal planes is also a principal plane. For an orthotropic material, one only requires 9 constants for elasticity and 3 for thermal expansion and for diffusion. Most engineering materials fall into this category. It should be pointed out that existing industrial standards only allow for material characterisation to go as far as orthotropy [11, 12]. There is no standard that

applies to material more anisotropic than orthotropy. Examples of abuses of such standards will be illustrated later in Section 18 in the chapter in relation to the twill weave composites.

Further categorisation along the line is possible, e.g. transversely isotropic, cubically symmetric, isotropic, etc.. For thermal expansion and for diffusion problems, cubic symmetry implies isotropy.

The role of rotational symmetries in material categorisation has hardly been mentioned anywhere in the literature. In an unpublished article [13], the leading author established that the presence of a 180° rotational symmetry identifies the axis of rotation as a principal axis of the material. As a result, a material is monoclinic if there exists a 180° rotational symmetry in it. It is generally true that the plane perpendicular to a principal axis is a principal plane and vice versa. With this, it can be concluded that a 180° rotational symmetry about an axis is of the same effects as having a reflectional symmetry about the plane perpendicular to the axis of rotational symmetry, as far as material categorisation is concerned.

Apparently, existence of more rotational symmetries will bring further simplifications to the material characteristics. One can comfortably follow the line of reflectional symmetries without any problem. However, it should be stated that the equivalence between rotational and reflectional symmetries in terms of material categorisation should not be blindly extended to any other field of application. They are certainly not equivalent in geometric sense.

7. Material Characterisation

Having categorised a material, material characterisation becomes relevant. Same as categorisation, in order to characterise a material, one needs to specify an appropriate length scale at which the outcomes of the characterisation will be presented. Usually, homogeneity can be assumed at this scale, to be referred to as the upper length scale. The objective of micromechanical material characterisation is to obtain effective material properties of the material at the upper length scale from the properties of its constituents and the structure at a lower length scale. The objective of such exercises is to reduce the demand on testing the material at its upper length scale.

Micromechanical material characterisation can be achieved by analysing an appropriately formulated RVE or UC. The analyses involved are to simulate physical experiments through which desired effective material properties are measured. For instance, in order to determine the Young's modulus and the Poisson's ratios of the material in a specific direction, a uniaxial stress, uniform in the upper length scale, should be applied. For it to be effectively uniaxial stress, one has to ensure all other stress components in the same length scale vanish identically. Failing to obtain an effectively uniaxial stress state has been a typical error in such analyses in the literature. The immediate outcome of such analyses is effective strains in response to the stress

applied, very much like in the physical experiments. The effective material properties can then readily obtained according to their definitions. The effective Young's modulus is equal to the ratio between the applied effective stress and the obtained effective strain in the same direction. The ratios between the obtained strains in three directions will provide the Poisson's ratios.

Similarly, a shear modulus should be obtained under an effectively pure shear stress state. The simulation of this loading case tends to be more prone to mistakes. Among the publications on micromechanical analysis, nine out of ten of them tended to avoid involving shear, often without any reason.

The same considerations can be given to all other physical disciplines, e.g. the diffusion problem. A key rule to bear in mind is that any effective property should be obtained according to its physical definition. Micromechanical analysis is to provide a means of virtual testing and it is the user's responsibility that all required testing conditions are observed in the simulation as well as in the physical testing. In many ways, it should be a lot easier to observe these conditions in theoretical simulation than on the physical lab floor. Having said so, there are probably as many pitfalls in virtual testing as in physical testing where mistakes can be made. Right attitude is often the key to success and nothing of this kind is meant to be easily achievable through casual tampering.

8. RVEs and Unit Cells

When analyses are made to materials of micro/meso-structures at a lower length scale in order to determine their effective properties in an upper length scale, it is often necessary to resort to the concepts of representative volume elements (RVEs) or unit cells (UCs) at the lower length scale where analyses are conducted before the effective material properties in the upper length scale can be extracted. The terminologies of RVEs and UCs could be interchanged sometimes, resulting in a degree of confusion. It is therefore helpful for the subsequent discussion if they are logically defined as follows.

8.1   RVEs

A representative volume element (RVE) is volume of the material of a size large enough so that any volume of an increased size will be equally representative. Apparently, for computational efficiency, one will be naturally interested in the minimum size of the RVE. Any volume of the material of a size smaller than that will no longer be representative. The minimum size of RVE may vary from material to material, from discipline to discipline, and sometimes from one effective property of interest to another. For instance, some properties, such as heat capacity, Young's modulus of unidirectional fibre reinforced composites (UD) in the fibre direction, etc., are dominated by the constituent volume fractions. For them, any RVE of the right volume

fraction will serve the purpose. Other properties might need a substantial chunk of the material in order to be representative, especially those based on statistical homogeneity.

The representativeness of an RVE is judged based on the effective properties it characterises. It does not have to be able to reproduce the appearance of any other parts of the material geometrically. In particular, when the lower length scale structure is at random, no part can possibly be reproduced by any other part. Even so, an appropriate RVE can be defined as long as the size of the RVE has been chosen large enough.

When introducing RVEs for random structures, such as that in Figure 6(a), at lower length scales, there is a practice which has been rather common but fundamentally wrong. In order to falsify periodicity so that periodic boundary condition can be imposed, truncated features on one side of the RVE are artificially moved to the opposite side and kept within the RVE, as shown in Figure 6(b). There are three obvious and fundamental issues associated with this practice.
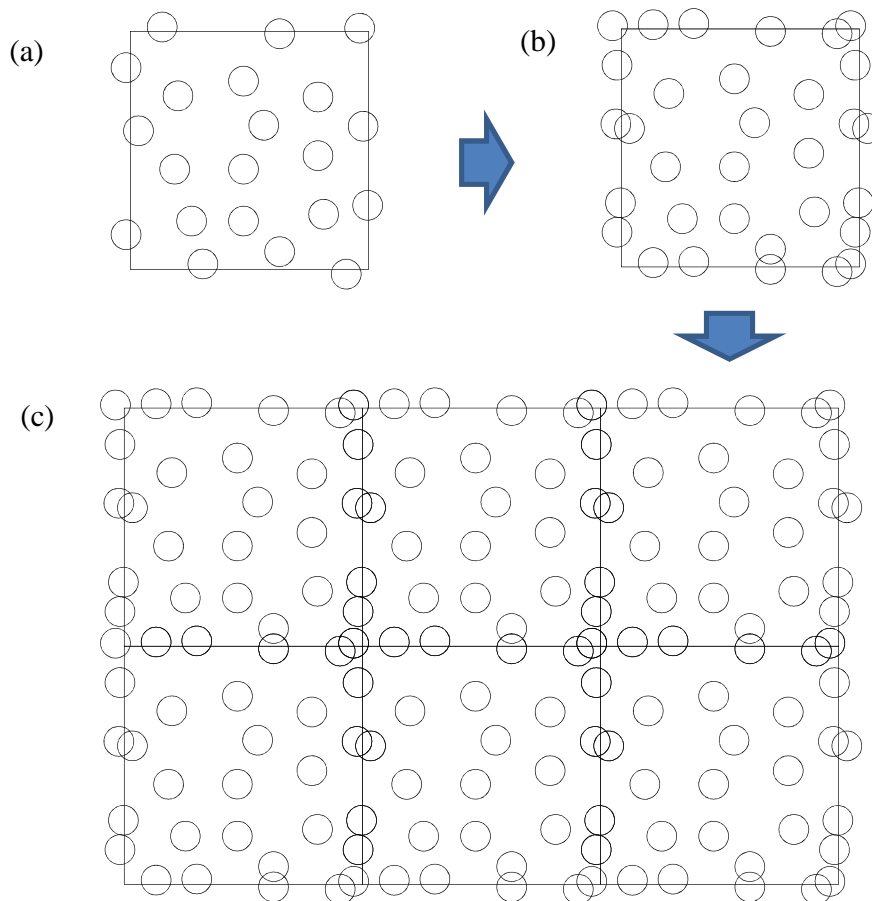

Figure 6 (a) RVE of a random structure; (b) tampered RVE; and (c) the material represented by the RVE

    a)   This interferes the constituent volume fractions, compromising its representativeness.

b) There is not always space available to accommodate the truncated features. The truncated features can only be dealt with by a number of means: (i) selecting specific patch where space happens to be available; (ii) allowing overlapping; (iii) artificially moving existing features around order to free some space; and (iv) artificially deleting overlapping features. In each case, the randomness of the structure will be undermined.

c) The falsified periodicity means periodicity in the structure at the length scale concerned, which can be seen if one lays up an array of such RVEs, see Figure 6(c). This spoils the randomness of the structure completely. With the structure so systematically tampered, one should question if it is still worthwhile to model such an RVE with the features seemingly distributed at random but no longer representative anymore in many ways.

It should be pointed out that appropriate approach to analyse untampered RVEs is available as will be addressed in one of the subsequent sections in the chapter.

8.2   UCs

A unit cell (UC) on the other hand is a portion of material which is meant to be able to reproduce all other parts of the material through some appropriate symmetry transformations, so that the UC and its duplicates can fill up the space the material occupies fully without leaving any gap or overlap. Here, the presence of a symmetry depends not only on the geometry but also on the physical considerations, e.g. loading conditions. Similar to RVEs, one is interested in the minimum size of the UC for a given material. In order to define a UC, it is essential that the regularity is present in the structure. Otherwise, UCs are simply inapplicable.

The definition of a UC relies on correct interpretation of symmetries present in the structure. It should be pointed out that even for the same pattern, unit cells of different appearances can be obtained. Sometimes, building blocks are naturally partitioned, such as fish scale pavement tiles in the 2D case as shown in Figure 7(a). Otherwise, as a generally applicable approach, the Voronoi diagram [14] as shown in Figure 7(b) can be employed to tessellate the patterned structure. A Voronoi cell is generated in such a way that each side of it perpendicularly bisects the segment connecting the centres of the adjacent cells. Just as they represent the same physical problem, different shapes of the UC follow the same translational symmetries and therefore they should result in exactly the same outcomes in terms of stress distribution in the lower length scale and effective properties in the upper scale [4].

Having dismissed the significance of the differences in the appearances of UCs, readers are reminded one aspect of practicality. When the UCs are analysed eventually, in particular, using finite elements, different choices of the shapes could make significant differences to the generation and quality of the meshes. Some choices could leave awkward areas in the UC to mesh, e.g. those involving extremely sharp corners. It is therefore advisable that serious users of UCs ought to be 'mesh-minded' when deciding the shape of the UC to be employed.

Once the shape of a UC has been selected one way or another, the boundary of the UC has been determined. Sorting out the correspondence between various parts of the boundary associated with the translational symmetries present in the structure in the relevant length scale is a key step.
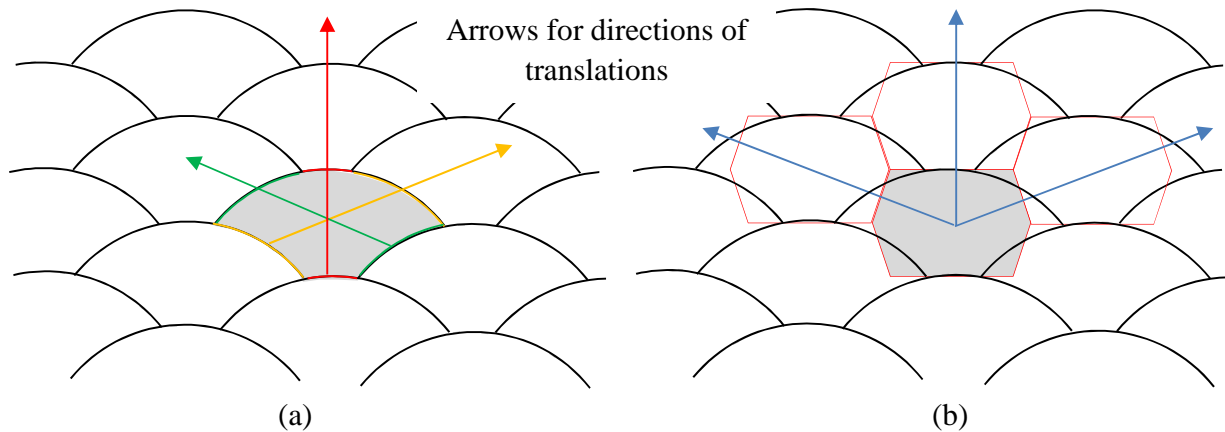

Figure 7 Unit cells of different shapes for the same pattern

Consider the 2D pattern in Figure 7 for example, whilst the concept can be readily extended to 3D or reduced to 1D applications. In this case, each translational symmetry defines a pair of segments (patches for 3D cases) of the boundary which are the original and the image under the translational symmetry transformation. The three pairs involved in the present example, indicated in coloured segments in Figure 7(a), are associated with the three directions of translations marked using the same colour codes, but there could be more (in particular, in 3D cases) or fewer pairs, in general, without changing the principles at all. These translational symmetries will lead to relationships of displacements between each pair of segments. These relationships define the boundary conditions for the unit cell. Formulation of boundary conditions for a UC proves to be the most challenging task in the construction of the UC. A systematic account on the boundary conditions will be present later in the chapter.

With properly formulated boundary conditions, there will never be a need to analyse an assembly of an array of unit cells, as has sometimes been seen in the literature [15], since they should result in identical outcomes. Any attempt of doing so gives a clear sign of incompetence in using UCs and automatically casts doubt on the results obtained.

In the literature, another terminology, representative unit cells (RUCs), is sometimes seen. This was probably intended to reconcile between RVEs and UCs but it does not help as it leads to more confusion. A logic reconciliation between RVEs and UCs it that a UC is always an RVE but not vice versa. In this sense, RUC is in fact tautology as buttery butter.

In terms of applications, UCs and RVEs are designated for regular and random micro/meso structures, respectively. The leading author wishes to confess that, in his publications in the past, he did not follow this rule of classification, e.g. [16,17]. The classification suggested above only became clear in his vision afterwards when more thought had been given to this issue in order to be logical as much as possible.

9. Relative Displacement Field

A typical multiscale modelling involves two length scales, an upper one and a lower one. The objective of material characterisation using multiscale modelling is usually to evaluate the effective material properties in the upper scale based on the analyses conducted with the models at the lower scale. The basic assumptions made to the material at upper scale are that it is effectively homogeneous and the stress and strain states prescribed to it are both uniform. The homogeneity here can be justified either in a statistical sense or based on the periodicity in the structure at the lower scale. Correspondingly, RVEs or UCs will be resorted to in order to facilitate the analysis at the lower scale. To obtain the effective properties, one has to follow their definitions to evaluate them from the uniform stresses and the uniform strains at upper scale. Between the two sets of values, uniform stresses and uniform strains, if one employs one as the means of prescribing the loads to the RVE or UC to be analysed, the other will be a part of the results out of the analysis. To follow the definition of effective properties in their form of engineering constants, e.g. Young's moduli, Poisson's ratio and shear moduli, it is necessary that the material is loaded in its upper scale with a uniaxial stress states or a pure shear stress state. It is therefore usually more convenient if such loading conditions can be prescribed. In return, strains in the upper scale can be obtained as a part of the results. This is a procedure very similar to what one would follow if these properties had to be measured experimentally. The material characterisation using RVEs or UCs is therefore a genuine case of virtual testing.

Having sorted out various relationships at the upper scale, the analysis has to be conducted at the lower scale. A crucial link across both scales is the relationship between the lower scale displacement field and the upper scale strains. In this respect, RVEs will be addressed later separately. Discussion below will be focused on UCs for the time being.

In this case, the regularity in the lower scale structure is assumed. The upper scale homogeneity is based on the existence of translational symmetries in three dimensions, not necessarily along the coordinate axes. As discussed in Section 5, the translational symmetry is present in the relative displacement field, i.e.

$$\left\{ \begin{array}{c} u \\ v \\ w \end{array} \right\}\bigg|_{(x,y.z)} - \left\{ \begin{array}{c} u \\ v \\ w \end{array} \right\}\bigg|_{R} = \left\{ \begin{array}{c} u \\ v \\ w \end{array} \right\}\bigg|_{(x',y',z')} - \left\{ \begin{array}{c} u \\ v \\ w \end{array} \right\}\bigg|_{R'}, \tag{27}$$

24

where point (x',y',z') and R' are, respectively, the image of an arbitrary point (x,y,z) within the UC concerned and a reference point R which is a fixed point within the UC under a translational symmetry transformation. The translation can be described in the coordinates of an arbitrary point and its image after the translation as follows.

$$
\begin{Bmatrix} x' \\ y' \\ z' \end{Bmatrix} = \begin{Bmatrix} x \\ y \\ z \end{Bmatrix} + \begin{Bmatrix} \Delta x \\ \Delta y \\ \Delta z \end{Bmatrix} \quad \text{and} \quad \begin{Bmatrix} x \\ y \\ z \end{Bmatrix}\Bigg|_{R'} = \begin{Bmatrix} x \\ y \\ z \end{Bmatrix}\Bigg|_{R} + \begin{Bmatrix} \Delta x \\ \Delta y \\ \Delta z \end{Bmatrix}, \tag{28}
$$

where

$$
\begin{Bmatrix} \Delta x \\ \Delta y \\ \Delta z \end{Bmatrix} = \sum_{i=1}^{k} \Delta_i \mathbf{q}_i .
$$

Here Δ_i ($i = 1.. k$) are the distances of translations involved, with k being the number of independent directions of translational symmetries defined by unit vectors $\mathbf{q}_i$, respectively. Rearranging (27), one obtains the relative displacement field as

$$
\begin{Bmatrix} u \\ v \\ w \end{Bmatrix}\Bigg|_{(x',y',z')} - \begin{Bmatrix} u \\ v \\ w \end{Bmatrix}\Bigg|_{(x,y,z)} = \begin{Bmatrix} u \\ v \\ w \end{Bmatrix}\Bigg|_{R'} - \begin{Bmatrix} u \\ v \\ w \end{Bmatrix}\Bigg|_{R} . \tag{29}
$$

Since points R and R' are located at the same place inside respective unit cell, they can be employed to construct the uniform strain filed in the upper scale. The relative displacements between these two points in the lower scale in each respective unit cell should be the same as the relative displacements (U, V, W) in the upper scale, i.e.

$$
\begin{Bmatrix} u \\ v \\ w \end{Bmatrix}\Bigg|_{R'} - \begin{Bmatrix} u \\ v \\ w \end{Bmatrix}\Bigg|_{R} = \begin{Bmatrix} U \\ V \\ W \end{Bmatrix}\Bigg|_{R'} - \begin{Bmatrix} U \\ V \\ W \end{Bmatrix}\Bigg|_{R} = \begin{Bmatrix} \Delta U \\ \Delta V \\ \Delta W \end{Bmatrix} . \tag{30}
$$

According to deformation kinematics, the relative displacement field in the upper length scale corresponding to a uniform strain field can be obtained through the displacement gradient in general as

$$
\left\{
\begin{array}{c}
\Delta U \\
\Delta V \\
\Delta W
\end{array}
\right\} =
\begin{bmatrix}
\dfrac{\partial U}{\partial x} & \dfrac{\partial U}{\partial y} & \dfrac{\partial U}{\partial z} \\[2ex]
\dfrac{\partial V}{\partial x} & \dfrac{\partial V}{\partial y} & \dfrac{\partial V}{\partial z} \\[2ex]
\dfrac{\partial W}{\partial x} & \dfrac{\partial W}{\partial y} & \dfrac{\partial W}{\partial z}
\end{bmatrix}
\left\{
\begin{array}{c}
\Delta x \\
\Delta y \\
\Delta z
\end{array}
\right\}.
\tag{31}
$$

In its general form, displacement gradient (31) describes fully the change in shape of the body and the rotation as a rigid body. In conventional stress analysis, one is interested in the deformation primarily, i.e. a part of (31), whilst the rigid body rotation can be left aside. To facilitate this, displacement gradient is conventionally partitioned into a symmetric and an antisymmetric part as follows and the symmetric part gives the strain tensor under the assumption of small deformation (strains are defined differently under finite deformation involving higher order terms according to the definition of Green strain as a tensor).

$$
\begin{bmatrix}
\dfrac{\partial U}{\partial x} & \dfrac{\partial U}{\partial y} & \dfrac{\partial U}{\partial z} \\[2ex]
\dfrac{\partial V}{\partial x} & \dfrac{\partial V}{\partial y} & \dfrac{\partial V}{\partial z} \\[2ex]
\dfrac{\partial W}{\partial x} & \dfrac{\partial W}{\partial y} & \dfrac{\partial W}{\partial z}
\end{bmatrix} =
\begin{bmatrix}
\varepsilon_x^0 & \varepsilon_{xy}^0 & \varepsilon_{xz}^0 \\
\varepsilon_{xy}^0 & \varepsilon_y^0 & \varepsilon_{yz}^0 \\
\varepsilon_{xz}^0 & \varepsilon_{yz}^0 & \varepsilon_z^0
\end{bmatrix} +
\begin{bmatrix}
0 & -\omega_{xy}^0 & \omega_{xz}^0 \\
\omega_{xy}^0 & 0 & -\omega_{yz}^0 \\
-\omega_{xz}^0 & \omega_{yz}^0 & 0
\end{bmatrix},
\tag{32}
$$

where

$$
\left[\varepsilon^0\right] =
\begin{bmatrix}
\varepsilon_x^0 & \varepsilon_{xy}^0 & \varepsilon_{xz}^0 \\
\varepsilon_{xy}^0 & \varepsilon_y^0 & \varepsilon_{yz}^0 \\
\varepsilon_{xz}^0 & \varepsilon_{yz}^0 & \varepsilon_z^0
\end{bmatrix} =
\begin{bmatrix}
\dfrac{\partial U}{\partial x} & \dfrac{1}{2}\left(\dfrac{\partial V}{\partial x}+\dfrac{\partial U}{\partial y}\right) & \dfrac{1}{2}\left(\dfrac{\partial U}{\partial z}+\dfrac{\partial W}{\partial x}\right) \\[2ex]
\dfrac{1}{2}\left(\dfrac{\partial V}{\partial x}+\dfrac{\partial U}{\partial y}\right) & \dfrac{\partial V}{\partial y} & \dfrac{1}{2}\left(\dfrac{\partial W}{\partial y}+\dfrac{\partial V}{\partial z}\right) \\[2ex]
\dfrac{1}{2}\left(\dfrac{\partial U}{\partial z}+\dfrac{\partial W}{\partial x}\right) & \dfrac{1}{2}\left(\dfrac{\partial W}{\partial y}+\dfrac{\partial V}{\partial z}\right) & \dfrac{\partial W}{\partial z}
\end{bmatrix}
\tag{33}
$$

is the strain tensor which happens to be uniform in the upper scale in the present problem, and

$$
\left\{
\begin{array}{c}
\omega_{yz}^0 \\
\omega_{xz}^0 \\
\omega_{xy}^0
\end{array}
\right\} = \frac{1}{2}
\left\{
\begin{array}{c}
\dfrac{\partial W}{\partial y}-\dfrac{\partial V}{\partial z} \\[2ex]
\dfrac{\partial U}{\partial z}-\dfrac{\partial W}{\partial x} \\[2ex]
\dfrac{\partial V}{\partial x}-\dfrac{\partial U}{\partial y}
\end{array}
\right\}
\tag{34}
$$

is the rotation vector as a part of the displacement field in the upper scale. In fact, these rotations can be visualised as follows. Generate three straight lines, one on each of the three coordinate planes at 45 degrees (denoted as 45 in the superscripts for expressions to follow) to the coordinate axes on both sides of it. The components of the rotation vector above give the rotation of each of these lines about the coordinate axis perpendicular to the line, e.g. the line on the *x-y* plane about the *z*-axis, so on. These rotations can be denoted as

$$
\left\{ R^{45°} \right\} = \begin{Bmatrix} R_x^{45°} \\ R_y^{45°} \\ R_z^{45°} \end{Bmatrix} = \begin{Bmatrix} \omega_{yz}^0 \\ \omega_{xz}^0 \\ \omega_{xy}^0 \end{Bmatrix} = \frac{1}{2} \begin{Bmatrix} \dfrac{\partial W}{\partial y} - \dfrac{\partial V}{\partial z} \\[2mm] \dfrac{\partial U}{\partial z} - \dfrac{\partial W}{\partial x} \\[2mm] \dfrac{\partial V}{\partial x} - \dfrac{\partial U}{\partial y} \end{Bmatrix}. \tag{35}
$$

For material characterisation, one is also only interested in deformation part of the displacement gradient whilst the rotation part does not make any difference. Given the partition in (32), it is apparently a straightforward way of expressing the relative displacement field by dropping the rotation part while keeping the strain part, i.e.

$$
\begin{Bmatrix} u \\ v \\ w \end{Bmatrix}\Bigg|_{(x',y',z')} - \begin{Bmatrix} u \\ v \\ w \end{Bmatrix}\Bigg|_{(x,y.z)} = \begin{bmatrix} \varepsilon_x^0 & \varepsilon_{xy}^0 & \varepsilon_{xz}^0 \\ \varepsilon_{xy}^0 & \varepsilon_y^0 & \varepsilon_{yz}^0 \\ \varepsilon_{xz}^0 & \varepsilon_{yz}^0 & \varepsilon_z^0 \end{bmatrix} \begin{Bmatrix} \Delta x \\ \Delta y \\ \Delta z \end{Bmatrix}. \tag{36}
$$

Effectively, this is to eliminate the rigid body rotations by constraining the rotation of each of the three 45° lines as described above. It is clear that dropping the second term from (32) is equivalent to constraining rigid body rotations in the specific way.

Although partitioning the displacement gradient as defined by (32) is perfectly legitimate, one should not perceive that this is the only way of associating the relative displacement field with the strains. It can be shown that a more general form of partitioning the displacement gradient can be given as

$$
\begin{Bmatrix} \Delta U \\ \Delta V \\ \Delta W \end{Bmatrix} = \begin{bmatrix} \dfrac{\partial U}{\partial x} & \dfrac{\partial U}{\partial y} & \dfrac{\partial U}{\partial z} \\[2mm] \dfrac{\partial V}{\partial x} & \dfrac{\partial V}{\partial y} & \dfrac{\partial V}{\partial z} \\[2mm] \dfrac{\partial W}{\partial x} & \dfrac{\partial W}{\partial y} & \dfrac{\partial W}{\partial z} \end{bmatrix} \begin{Bmatrix} \Delta x \\ \Delta y \\ \Delta z \end{Bmatrix} = [F] \begin{Bmatrix} \Delta x \\ \Delta y \\ \Delta z \end{Bmatrix} + [\Omega] \begin{Bmatrix} \Delta x \\ \Delta y \\ \Delta z \end{Bmatrix}, \tag{37}
$$

where

$$[F] = \begin{bmatrix} \varepsilon_x^0 & k_3\varepsilon_{xy}^0 & k_2\varepsilon_{xz}^0 \\ (2-k_3)\varepsilon_{xy}^0 & \varepsilon_y^0 & k_1\varepsilon_{yz}^0 \\ (2-k_2)\varepsilon_{xz}^0 & (2-k_1)\varepsilon_{yz}^0 & \varepsilon_z^0 \end{bmatrix} \begin{Bmatrix} \Delta x \\ \Delta y \\ \Delta z \end{Bmatrix} \tag{38}$$

$$[\Omega] = \begin{bmatrix} 0 & -\dfrac{1}{2}k_3\dfrac{\partial V}{\partial x}+\left(1-\dfrac{1}{2}k_3\right)\dfrac{\partial U}{\partial y} & -\dfrac{1}{2}k_2\dfrac{\partial W}{\partial x}+\left(1-\dfrac{1}{2}k_2\right)\dfrac{\partial U}{\partial z} \\ \dfrac{1}{2}k_3\dfrac{\partial V}{\partial x}-\left(1-\dfrac{1}{2}k_3\right)\dfrac{\partial U}{\partial y} & 0 & -\dfrac{1}{2}k_1\dfrac{\partial W}{\partial y}+\left(1-\dfrac{1}{2}k_1\right)\dfrac{\partial V}{\partial z} \\ \dfrac{1}{2}k_2\dfrac{\partial W}{\partial x}-\left(1-\dfrac{1}{2}k_2\right)\dfrac{\partial U}{\partial z} & \dfrac{1}{2}k_1\dfrac{\partial W}{\partial y}-\left(1-\dfrac{1}{2}k_1\right)\dfrac{\partial V}{\partial z} & 0 \end{bmatrix}. \tag{39}$$

where k_i (i=1..3) can be arbitrary constants as long as they do not compromise the small deformation assumption with one exception as will be discussed later. It can be observed that $[\Omega]$ vanishes if

$$k_1\frac{\partial W}{\partial y}=(2-k_1)\frac{\partial V}{\partial z}$$

$$k_2\frac{\partial W}{\partial x}=(2-k_2)\frac{\partial U}{\partial z} \tag{40}$$

$$k_3\frac{\partial V}{\partial x}=(2-k_3)\frac{\partial U}{\partial y}$$

Take the third equation above for instance and consider a rectangle in the *x-y* plane before deformation as shown in dashed line in Figure 8. It deforms into a parallelogram as shown in Figure 8 in solid line. $\dfrac{\partial V}{\partial x}$ and $\dfrac{\partial U}{\partial y}$ are the angles of the rotations of the two sides due to deformation as indicated. The sum of them gives the shear strain the plane. The relative magnitudes of them can vary by rotating the parallelogram as a rigid body in the plane without affecting the strain state. At any given ratio between $\eta = \dfrac{\partial V}{\partial x}\Big/\dfrac{\partial U}{\partial y}$, a constant k_3 can be determined as $k_3 = \dfrac{2}{1+\eta}$ so that the third equation of (40) will be satisfied identically.

Alternatively, given an arbitrary value of k_3, the deformed body can be rotated as a rigid body about the *z*-axis such that the ratio between $\dfrac{\partial V}{\partial x}$ and $\dfrac{\partial U}{\partial y}$ is adjusted to $\dfrac{\partial V}{\partial x}:\dfrac{\partial U}{\partial y}=(2-k_3):k_3$.

One can determine k_1 and k_2 in a similar manner. Alternatively, for arbitrarily given values of k_1 and k_2, one can rotate the deformed body about *x* and *y* axes, respectively, so that $[\Omega]$ will vanish. Then the relative displacement field can be expressed as
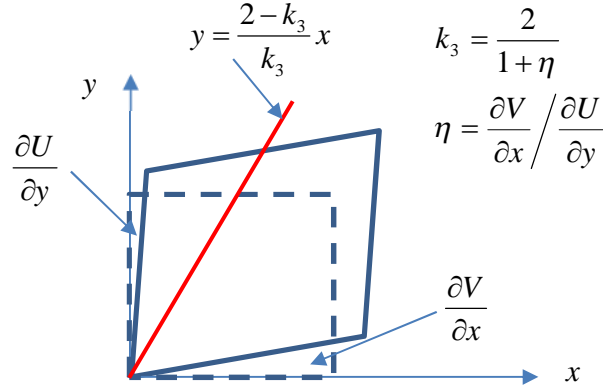
Figure 8 The line in the *x-y* plane that does not rotate as the body deforms for an arbitrarily given displacement gradient

$$
\begin{Bmatrix} \Delta U \\ \Delta V \\ \Delta W \end{Bmatrix} = \begin{bmatrix} \varepsilon_x^0 & k_3\varepsilon_{xy}^0 & k_2\varepsilon_{xz}^0 \\ (2-k_3)\varepsilon_{xy}^0 & \varepsilon_y^0 & k_1\varepsilon_{yz}^0 \\ (2-k_2)\varepsilon_{xz}^0 & (2-k_1)\varepsilon_{yz}^0 & \varepsilon_z^0 \end{bmatrix} \begin{Bmatrix} \Delta x \\ \Delta y \\ \Delta z \end{Bmatrix}. \tag{41}
$$

This captures the same strain field as that given by (31) or (36). The differences between them are up to some rigid body rotations. Taking the *x-y* plane as an example again, using k_3 as determined by the $\dfrac{\partial V}{\partial x}$ to $\dfrac{\partial U}{\partial y}$ ratio is equivalent to eliminating the rigid body rotation about the z-axis by constraining a line in the plane. To satisfy an enquiring mind, the line concerned here can be defined as $y = \dfrac{2-k_3}{k_3}x$. Using an arbitrary value of k_3 in (41), the line as shown in Figure 8 before deformation will rotate as a result of the deformation. Dropping the [Ω] term from (37) is equivalent to giving the deformed body a rigid body rotation so that the line after deformation lines up with that before deformation, which apparently will not alter the strain state. In this sense, [Ω] can also be considered as a rotation matrix defining the rotation of the line as shown Figure 8. As this additional rigid body rotation does not affect the strain state, it can be excluded from the consideration. Having excluded this rigid body rotation, using an arbitrary value of k_3 is equivalent to eliminating the rigid body rotation about the z-axis by constraining the $y = \dfrac{2-k_3}{k_3}x$ line in the *x-y* plane.

There is an apparent exception when $\dfrac{\partial V}{\partial x} = -\dfrac{\partial U}{\partial y}$, i.e. shear strain γ_{xy} vanishes. In this case, $\eta = -1$ and k_3 approaches infinity. The non-rotating line as shown in Figure 8 does not exist.

Anything associated with $\dfrac{\partial V}{\partial x}$ and $\dfrac{\partial U}{\partial y}$ amounts to a rigid body rotation. As far as this special case of exception is concerned, the line as shown in Figure 8 can be selected arbitrarily without affecting the strain state.

With the general form of partitioning the displacement gradient as established in (37)-(39), the rigid body rotations can be constrained in different ways from constraining $\left\{ R^{45°} \right\}$. Constraining the rigid body rotations of lines other than the 45° ones simply corresponds to assigning different values to k_i ($i=1..3$). It is now clear that the way of constraining the rigid body rotations is not unique. Any of them will be correct as long as it has been carried out logically.

If the extreme value of the 2 for all k_i ($i=1..3$) is taken, from (40) one obtains

$$
\left\{
\begin{array}{c}
\dfrac{\partial W}{\partial y} \\[2mm]
\dfrac{\partial W}{\partial x} \\[2mm]
\dfrac{\partial V}{\partial x}
\end{array}
\right\}
=
\left\{
\begin{array}{c}
0 \\ 0 \\ 0
\end{array}
\right\}.
\tag{42}
$$

The three components on the left hand side happen to correspond to the rotation of the y-axis about the x-axis, and those of the x-axis about the y- and z-axes, respectively. When they vanish, the rigid body rotations are eliminated. Effectively, this can be visualised as if these three axes have been constrained from the rotations as specified.

Following this way to eliminate rigid body rotations, using the engineering strains γ instead of tensor strains ε as in (33) and (35), the relative displacement field becomes

$$
\left.\left\{
\begin{array}{c} u \\ v \\ w \end{array}
\right\}\right|_{(x',y',z')}
-
\left.\left\{
\begin{array}{c} u \\ v \\ w \end{array}
\right\}\right|_{(x,y.z)}
=
\begin{bmatrix}
\dfrac{\partial U}{\partial x} & \dfrac{\partial U}{\partial y} & \dfrac{\partial U}{\partial z} \\[2mm]
0 & \dfrac{\partial V}{\partial y} & \dfrac{\partial V}{\partial z} \\[2mm]
0 & 0 & \dfrac{\partial W}{\partial z}
\end{bmatrix}
\left\{
\begin{array}{c} \Delta x \\ \Delta y \\ \Delta z \end{array}
\right\}
=
\begin{bmatrix}
\varepsilon_x^0 & \gamma_{xy}^0 & \gamma_{xz}^0 \\
0 & \varepsilon_y^0 & \gamma_{yz}^0 \\
0 & 0 & \varepsilon_z^0
\end{bmatrix}
\left\{
\begin{array}{c} \Delta x \\ \Delta y \\ \Delta z \end{array}
\right\}.
\tag{43}
$$

This does not violate any rules of deformation kinematics and therefore captures the same strain field as (31) or (36). However, the lack of unique expression for relative displacement field can easily become a source of confusion if one is driven merely by his/her intuition without due respect of the basics of deformation kinematics.

30

10. Relative Displacement Boundary Conditions for Unit Cells

Relative displacement field (43) provides the relationship between the displacements at corresponding points in different unit cells according to the translational symmetries present in the problem. Point (*x,y,z*) can be anywhere in the unit cell. When it is on the boundary with (*x',y',z'*) on another part of the boundary of the same unit cell, (43) delivers the *relative displacement boundary conditions* for the unit cell. As discussed in Section 8, the boundary of the unit cell has to be divided into parts in pairs with each pair associated with a translational symmetry. There should be neither gap nor overlap between these parts of the boundary.

Relative displacement boundary conditions have been called periodic boundary conditions [18]. However, while stress and strain fields are periodic in presence of translational symmetries, periodicity is simply not available in displacement field at all. Calling them the displacement boundary conditions by periodic boundary has undoubtedly been a source of confusion. Periodicity is observed in the relative displacement field. To avoid further confusion, especially for new unit cell users, it is suggested to call them as relative displacement boundary conditions.

Relative displacement boundary conditions involve displacements on two different parts of the boundary of the unit cell, which provide certain relationships between them. The relationships are in fact the definition of relative displacements, i.e. the differences between the displacements on the two parts of the boundary related through a translational symmetry of relative displacements. As established in the previous section, relative displacements can be related to the uniform strain field in the upper length scale. Unfortunately, as explained in the previous section, such expression is not unique. Here, relative displacement defined by (43) is chosen for subsequent applications, i.e.

$$\begin{Bmatrix} u' \\ v' \\ w' \end{Bmatrix} - \begin{Bmatrix} u \\ v \\ w \end{Bmatrix} = \begin{bmatrix} \varepsilon_x^0 & \gamma_{xy}^0 & \gamma_{xz}^0 \\ 0 & \varepsilon_y^0 & \gamma_{yz}^0 \\ 0 & 0 & \varepsilon_z^0 \end{bmatrix} \begin{Bmatrix} \Delta x \\ \Delta y \\ \Delta z \end{Bmatrix} . \tag{44}$$

The reason for the choice of (43) over (36) is purely based on the implementation consideration where equations imposing these conditions in the analysis will have fewer terms to be defined. For example, for the displacement in z-direction, using the above, one has

$$w' - w = \varepsilon_z^0 \Delta z \ , \tag{45}$$

whilst using (36), one would have

$$w' - w = \frac{1}{2} \gamma_{xz}^0 \Delta x + \frac{1}{2} \gamma_{yz}^0 \Delta y + \varepsilon_z^0 \Delta z . \tag{46}$$

The results in terms of obtained stress field in the lower length scale and the effective properties in the upper scale would be identical.

It should be pointed out that corresponding to each translational symmetry present in the structure, there is a different set of $\begin{pmatrix} \Delta x & \Delta y & \Delta z \end{pmatrix}$, which is the translation given as a vector, including the direction and the distance.

A range of unit cells both in 2D and 3D cases have been published in [4, 6, 17, 19]. Without repeating the details, they are categorised as follows.

10.1   2D unit cell with translational symmetries along coordinate axes

The simplest unit cell [5] for this is a rectangle with its side lengths corresponding to the distances of translations associated with the symmetries, as shown in Figure 9. A special case is the square unit cell. The relative displacement boundary conditions are given as
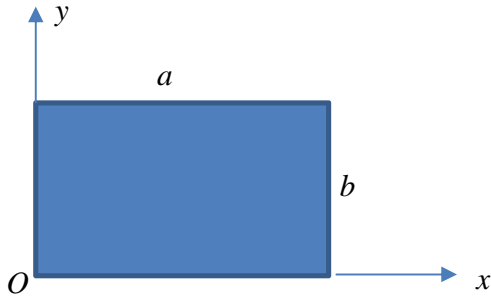

 Figure 9 Rectangular 2D unit cell

For the parts of the boundary perpendicular to the x axis, the relevant translation can be given as

$$\begin{Bmatrix} \Delta x \\ \Delta y \end{Bmatrix} = \begin{Bmatrix} a \\ 0 \end{Bmatrix} \tag{47}$$

and as a result, the relative displacement boundary conditions can be obtained from (44) as

$$u\big|_{x=a} - u\big|_{x=0} = \varepsilon_x^0 a$$
$$v\big|_{x=a} - v\big|_{x=0} = 0. \tag{48}$$

Similarly, the translation for the other pair of sides,

$$\begin{Bmatrix} \Delta x \\ \Delta y \end{Bmatrix} = \begin{Bmatrix} 0 \\ b \end{Bmatrix} \tag{49}$$

and hence

$$u\big|_{y=b} - u\big|_{y=0} = \gamma_{xy}^0 b$$
$$v\big|_{y=b} - v\big|_{y=0} = \varepsilon_y^0 b. \tag{50}$$

As both sets of boundary conditions apply to the corners, redundancies emerge. If the solver employed does not allow such redundancies in the boundary conditions, one will have to remove them manually. In order to do so, the above boundary conditions are imposed only to the sides with the corners excluded. A special set of boundary conditions as follows are imposed to the corners only.

$$u\big|_{(a,0)} - u\big|_{(0,0)} = \varepsilon_x^0 a$$
$$v\big|_{(a,0)} - v\big|_{(0,0)} = 0$$

corresponding to translation $\left\{\begin{matrix} \Delta x \\ \Delta y \end{matrix}\right\} = \left\{\begin{matrix} a \\ 0 \end{matrix}\right\}$,

$$u\big|_{(0,b)} - u\big|_{(0,0)} = \gamma_{xy}^0 b$$
$$v\big|_{(0,b)} - v\big|_{(0,0)} = \varepsilon_y^0 b$$

corresponding to translation $\left\{\begin{matrix} \Delta x \\ \Delta y \end{matrix}\right\} = \left\{\begin{matrix} 0 \\ b \end{matrix}\right\}$, (51)

$$u\big|_{(a,b)} - u\big|_{(0,0)} = \varepsilon_x^0 a + \gamma_{xy}^0 b$$
$$v\big|_{(a,b)} - v\big|_{(0,0)} = \varepsilon_y^0 b$$

corresponding to translation $\left\{\begin{matrix} \Delta x \\ \Delta y \end{matrix}\right\} = \left\{\begin{matrix} a \\ 0 \end{matrix}\right\} + \left\{\begin{matrix} 0 \\ b \end{matrix}\right\}$.

In imposing the above relative displacement conditions at the corners, attention needs to be paid to the actual approach employed in the specific FE code used. For instance, in Abaqus/Standard, such constrains are imposed by eliminating the first degree of freedom (dof) appearing in the equation. As some degrees of freedom tend to appear in multiple equations, the user must make sure that such a dof is not listed as the first in the equation. Otherwise, the execution of the analysis may abort in error as the eliminated dof in a previous condition cannot be eliminated again when it appears as the first dof the second time. A good practice is to keep such dofs away from the first in the dof list.

The most popular applications of square unit cells are for the analysis of UD composites with fibres arranged or idealised in a square packing, although readers are reminded that square fibre packing does not show transverse isotropy and therefore is not a suitable candidate if it is meant to be an idealisation of otherwise transversely isotropic material. Given this understanding, if transverse isotropy is deemed to be unimportant, the following boundary conditions can be used to facilitate the analysis after extending the 2D UC by adding a third dimension to it, with a translation distance along this direction being equal to t. For their direct relevance to UD applications, the coordinate system has been changed from the above such that the present one is in line with the conventional UD composites description.

$$u\big|_{x=t} - u\big|_{x=0} = t\varepsilon_x^0$$
$$v\big|_{x=t} - v\big|_{x=0} = 0$$
$$w\big|_{x=t} - w\big|_{x=0} = 0$$

$$u|_{y=b} - u|_{y=-b} = 2b\gamma_{xy}^0$$

$$v|_{y=b} - v|_{y=-b} = 2b\varepsilon_y^0 \qquad (52)$$

$$w|_{y=b} - w|_{y=-b} = 0$$

$$u|_{z=b} - u|_{z=-b} = 2b\gamma_{xz}^0$$

$$v|_{z=b} - v|_{z=-b} = 2b\gamma_{yz}^0$$

$$w|_{z=b} - w|_{z=-b} = 2b\varepsilon_z^0.$$

The above boundary conditions are given between paired faces. Redundant boundary conditions are present at the edges and vertices if they have been included as parts of the faces. If one wishes to eliminate them, the following procedure can be taken. Exclude the edges from faces and vertices from the edges. Impose the above boundary conditions to such defined faces first. The twelve edges can be put into groups, each having four edges parallel to one coordinate axis. In each group, anyone can reproduce the remaining three through translational symmetries available in the structure as have been employed to define the unit cell. Relating the displacements on the one to those at the remaining three results in only independent boundary conditions on such edges. Similar arguments can be applied to the vertices. Amongst all eight vertices, any one of them can reproduce the remaining seven through the translational symmetries available in the structure as have been employed to define the unit cell. Relating the displacements at the one to those at the remaining seven results in only independent boundary conditions at the vertices and hence helps to avoid undue redundancies.
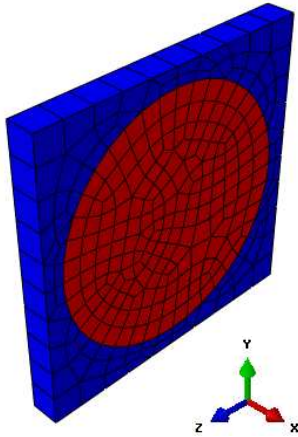

Figure 10 3D unit cell for UD composites of square packed fibres

A FE meshed square unit cell representing the UD composite is shown in Figure 10 [20,21]. One message it is intended to transmit is that one only needs a single layer of elements in the *x* direction, because correct results will not have any variation in stress field in this direction at all.

Having more layers of elements in this direction would make absolutely no difference, except an increased demand on computation. Any stress gradient observed in this direction will indicate an errors of some kind beyond doubt, most likely in the imposition of the boundary conditions. Such error can be easily diagnosed using the 'sanity checks' as will be described later in Section 15.

With a single layer of elements in the x direction, one might find that there is no node on any of the faces, having excluded the edges and vertices from them, if linear elements are employed. However, this does not undermine the significance of the boundary conditions obtained above for faces, as those for edges and vertices are all derived from them.

10.2   2D unit cell with translational symmetries along two non-orthogonal directions

This leads to unit cell of parallelogramatic shape as shown in Figure 11 [17]. Its side lengths are equal to the distances of translations associated with the symmetries. The relative displacement boundary conditions on the sides (excluding corners) are
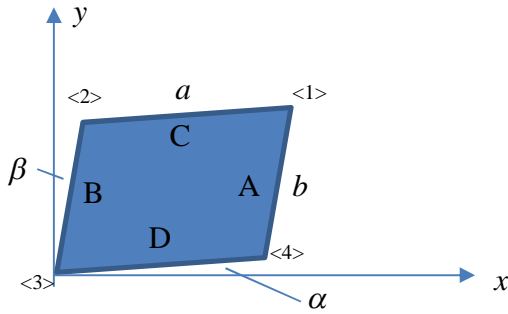

Figure 11 Unit cell of parallelogramatic shape

$$u\big|_A - u\big|_B = a\left(\varepsilon_x^0 \cos\alpha + \gamma_{xy}^0 \sin\alpha\right)$$
$$v\big|_A - v\big|_B = a\varepsilon_y^0 \sin\alpha$$

$$u\big|_C - u\big|_D = b\left(\varepsilon_x^0 \sin\beta + \gamma_{xy}^0 \cos\beta\right)$$
$$v\big|_C - v\big|_D = \varepsilon_y^0 b \cos\alpha,$$

(53)

whilst those at the corners are

$$u\big|_{\langle 4\rangle} - u\big|_{\langle 3\rangle} = a\left(\varepsilon_x^0 \cos\alpha + \gamma_{xy}^0 \sin\alpha\right)$$

$$v\big|_{\langle 4\rangle} - v\big|_{\langle 3\rangle} = a\varepsilon_y^0 \sin\alpha$$

$$u\big|_{\langle 2\rangle} - u\big|_{\langle 3\rangle} = b\left(\varepsilon_x^0 \sin\beta + \gamma_{xy}^0 \cos\beta\right)$$

$$v\big|_{\langle 2\rangle} - v\big|_{\langle 3\rangle} = \varepsilon_y^0 b\cos\alpha$$

$$u\big|_{\langle 1\rangle} - u\big|_{\langle 3\rangle} = \varepsilon_x^0\left(a\cos\alpha + b\sin\beta\right) + \gamma_{xy}^0\left(a\sin\alpha + b\cos\beta\right)$$

$$v\big|_{\langle 1\rangle} - v\big|_{\langle 3\rangle} = \varepsilon_y^0\left(a\sin\alpha + b\cos\alpha\right).$$

(54)

10.3   2D unit cell with translational symmetries along three different directions

The hexangular unit cell [5], Figure 12, rectangular unit cell from staggered layout [19], Figure 13, and that for the fish scale pattern as shown in Figure 7 all fall in this group. Although the shapes of them look rather different, they are topologically identical. Take the regular hexagonal unit cell for example, the relative displacement boundary conditions on the sides (excluding corners) are as follows with dashed and undashed displacements representing the sides after and before the corresponding translations in the direction as indicated by the arrows, respectively.
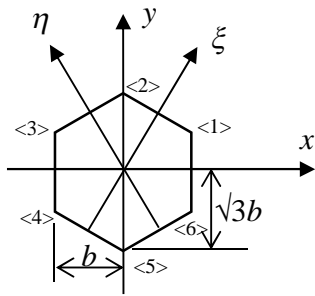

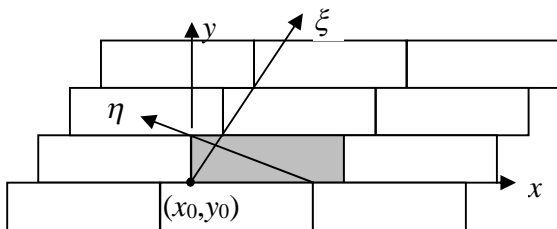Figure 12 Hexagonal unit cell with the directions of translations indicated

Figure 13 Unit cell for a staggered layout with the directions of translations indicated

Between the sides perpendicular to the x-axis, one has

$$u' - u = 2b\varepsilon_x^0$$
$$v' - v = 0.$$

(55)

Between the sides perpendicular to the ξ-axis (Figure 12), one has

$$u' - u = b\varepsilon_x^0 + \sqrt{3}b\gamma_{xy}^0$$
$$v' - v = \sqrt{3}b\varepsilon_y^0.$$

(56)

Between the sides perpendicular to the η-axis (Figure 12), one has

$$u' - u = -b\varepsilon_x^0 + \sqrt{3}b\gamma_{xy}^0$$
$$v' - v = \sqrt{3}b\varepsilon_y^0.$$

(57)

Those for the corners, after eliminating any redundant conditions, are

$$-u_{\langle 3 \rangle} + u_{\langle 1 \rangle} = 2b\varepsilon_x^0$$
$$-v_{\langle 3 \rangle} + v_{\langle 1 \rangle} = 0$$

$$-u_{\langle 5 \rangle} + u_{\langle 1 \rangle} = b\varepsilon_x^0 + \sqrt{3}b\gamma_{xy}^0$$
$$-v_{\langle 5 \rangle} + v_{\langle 1 \rangle} = \sqrt{3}b\varepsilon_y^0$$

(58)

$$u_{\langle 2 \rangle} - u_{\langle 4 \rangle} = 2b\varepsilon_x^0$$
$$v_{\langle 2 \rangle} - v_{\langle 4 \rangle} = 0$$

$$u_{\langle 6 \rangle} - u_{\langle 4 \rangle} = b\varepsilon_x^0 + \sqrt{3}b\gamma_{xy}^0$$
$$v_{\langle 6 \rangle} - v_{\langle 4 \rangle} = \sqrt{3}b\varepsilon_y^0.$$

Here the dofs at corner <1> have swapped positions with those on other nodes because they appeared in more than one equation. In addition to the above constraints, one can also relate corners <3> and <5>, but the constraints obtained would not be independent, neither will be those between corners <2> and <6>. Such dependent conditions, if imposed in some code such as Abaqus/Standard, could result in error for the reason as described earlier. It is a good practice to avoid them, although in some codes, e.g. Abaqus/Explicit, they are acceptable due to the explicit algorithm adopted.

As is for the square UC, the most popular applications of hexagonal unit cells are for the analysis of UD composites with fibres arranged or idealised in a hexagonal packing, which preserves the transverse isotropy perfectly. A third dimension has been incorporated in order to obtain the behaviour of the material in 3D [20,21]. The coordinate system has therefore been adapted to comply with conventional UD composites description, as shown in Figure 14, where only a single layer of elements is required as explained above for square UC.

Hexagon:

$$u\big|_{x=t} - u\big|_{x=0} = t\varepsilon_x^0$$
$$v\big|_{x=t} - v\big|_{x=0} = 0$$
$$w\big|_{x=t} - w\big|_{x=0} = 0$$

$$u\big|_{y=b} - u\big|_{y=-b} = 2b\gamma_{xy}^0$$
$$v\big|_{y=b} - v\big|_{y=-b} = 2b\varepsilon_y^0 \qquad\qquad (59)$$
$$w\big|_{y=b} - w\big|_{y=-b} = 0$$

$$u\big|_{\eta=b} - u\big|_{\eta=-b} = b\gamma_{xy}^0 + \sqrt{3}b\gamma_{xz}^0$$
$$v\big|_{\eta=b} - v\big|_{\eta=-b} = b\varepsilon_y^0 + \sqrt{3}b\gamma_{yz}^0$$
$$w\big|_{\eta=b} - w\big|_{\eta=-b} = \sqrt{3}b\varepsilon_z^0$$

$$u\big|_{\lambda=b} - u\big|_{\lambda=-b} = -b\gamma_{xy}^0 + \sqrt{3}b\gamma_{xz}^0$$
$$v\big|_{\lambda=b} - v\big|_{\lambda=-b} = -b\varepsilon_y^0 + \sqrt{3}b\gamma_{yz}^0$$
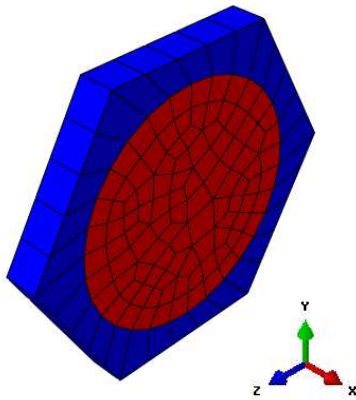$$w\big|_{\lambda=b} - w\big|_{\lambda=-b} = \sqrt{3}b\varepsilon_z^0.$$

Figure 14 3D unit cell for UD composites of hexagonally packed fibres

If one needs to avoid redundant boundary conditions along edges and at vertices, one can put the eighteen edges into four groups: all in x direction as one group and the remaining edges on the front and back faces into three groups, each having four edges parallel to each other. There are twelve vertices, at the ends of six edges in the x direction. They can be put in two groups, six in each. Each group is associated with three alternating edges in the x direction. The grouping of edges and vertices is so made that within each group any one can reproduce all the rest through the translational symmetries available in establish this UC. When the boundary conditions are prescribed to each group according to the translational symmetries by relating one vertex to the rest in the group, no redundancy will be introduced.

10.4   3D unit cell with translational symmetries along three non-coplanar axes

For materials of translational symmetries along three non-coplanar axes, the simplest shape for the unit cell is a parallelepiped with its side lengths corresponding to the distances of translations associated with the symmetries. A special case is a cuboidal unit cell [6] as shown in Figure 15 which will be taken as an example to illustrate the relative displacement boundary conditions.

For 3D unit cell, in order to avoid prescribing redundant conditions, the faces (excluding edges), edges (excluding vertices) and vertices need to be addressed separately.
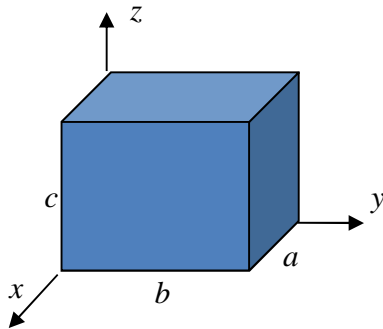

Figure 15 Cuboidal unit cell

For faces $x=0$ and $x=a$ (excluding edges)

$$u\big|_{x=a} - u\big|_{x=0} = a\varepsilon_x^0$$
$$v\big|_{x=a} - v\big|_{x=0} = 0 \tag{60}$$
$$w\big|_{x=a} - w\big|_{x=0} = 0.$$

39

For faces $y=0$ and $y=b$ (excluding edges)

$$\begin{aligned}
u\big|_{y=b} - u\big|_{y=0} &= b\gamma_{xy}^0 \\
v\big|_{y=b} - v\big|_{y=0} &= b\varepsilon_y^0 \\
w\big|_{y=b} - w\big|_{y=0} &= 0.
\end{aligned} \tag{61}$$

For faces $z=0$ and $z=c$ (excluding edges)

$$\begin{aligned}
u\big|_{z=c} - u\big|_{z=0} &= c\gamma_{xz}^0 \\
v\big|_{z=c} - v\big|_{z=0} &= c\gamma_{yz}^0 \\
w\big|_{z=c} - w\big|_{z=0} &= c\varepsilon_z^0.
\end{aligned} \tag{62}$$

For edges parallel to the x-axis (excluding vertices)

$$\begin{aligned}
u\big|_{y=b,z=0} - u\big|_{y=0,z=0} &= b\gamma_{xy}^0 \\
v\big|_{y=b,z=0} - v\big|_{y=0,z=0} &= b\varepsilon_y^0 \\
w\big|_{y=b,z=0} - w\big|_{y=0,z=0} &= 0 \\
u\big|_{y=0,z=c} - u\big|_{y=0,z=0} &= c\gamma_{xz}^0 \\
v\big|_{y=0,z=c} - v\big|_{y=0,z=0} &= c\gamma_{yz}^0 \\
w\big|_{y=0,z=c} - w\big|_{y=0,z=0} &= c\varepsilon_z^0 \\
u\big|_{y=b,z=c} - u\big|_{y=0,z=0} &= b\gamma_{xy}^0 + c\gamma_{xz}^0 \\
v\big|_{y=b,z=c} - v\big|_{y=0,z=0} &= b\varepsilon_y^0 + c\gamma_{yz}^0 \\
w\big|_{y=b,z=c} - w\big|_{y=0,z=0} &= c\varepsilon_z^0.
\end{aligned} \tag{63}$$

For edges parallel to the y-axis (excluding vertices), after eliminating any redundant conditions

$$\begin{aligned}
u\big|_{x=a,z=0} - u\big|_{x=0,z=0} &= a\varepsilon_x^0 \\
v\big|_{x=a,z=0} - v\big|_{x=0,z=0} &= 0 \\
w\big|_{x=a,z=0} - w\big|_{x=0,z=0} &= 0 \\
u\big|_{x=0,z=c} - u\big|_{x=0,z=0} &= c\gamma_{xz}^0 \\
v\big|_{x=0,z=c} - v\big|_{x=0,z=0} &= c\gamma_{yz}^0 \\
w\big|_{x=0,z=c} - w\big|_{x=0,z=0} &= c\varepsilon_z^0
\end{aligned} \tag{64}$$

$$u\big|_{x=a,z=c} - u\big|_{x=0,z=0} = a\varepsilon_x^0 + c\gamma_{xz}^0$$

$$v\big|_{x=a,z=c} - v\big|_{x=0,z=0} = c\gamma_{yz}^0$$

$$w\big|_{x=a,z=c} - w\big|_{x=0,z=0} = c\varepsilon_z^0.$$

For edges parallel to the *z*-axis (excluding vertices), after eliminating any redundant conditions

$$u\big|_{x=a,y=0} - u\big|_{x=0,y=0} = a\varepsilon_x^0$$

$$v\big|_{x=a,y=0} - v\big|_{x=0,y=0} = 0$$

$$w\big|_{x=a,y=0} - w\big|_{x=0,y=0} = 0$$

$$u\big|_{x=0,y=b} - u\big|_{x=0,y=0} = b\gamma_{xy}^0$$

$$v\big|_{x=0,y=b} - v\big|_{x=0,y=0} = b\varepsilon_y^0$$ (65)

$$w\big|_{x=0,y=b} - w\big|_{x=0,y=0} = 0$$

$$u\big|_{x=a,y=b} - u\big|_{x=0,y=0} = a\varepsilon_x^0 + b\gamma_{xy}^0$$

$$v\big|_{x=a,y=b} - v\big|_{x=0,y=0} = b\varepsilon_y^0$$

$$w\big|_{x=a,y=b} - w\big|_{x=0,y=0} = 0.$$

For the vertices, after eliminating any redundant conditions, one has

$$u\big|_{x=a,y=0,z=0} - u\big|_{x=0,y=0,z=0} = a\varepsilon_x^0$$

$$v\big|_{x=a,y=0,z=0} - v\big|_{x=0,y=0,z=0} = 0$$

$$w\big|_{x=a,y=0,z=0} - w\big|_{x=0,y=0,z=0} = 0$$

$$u\big|_{x=0,y=b,z=0} - u\big|_{x=0,y=0,z=0} = b\gamma_{xy}^0$$

$$v\big|_{x=0,y=b,z=0} - v\big|_{x=0,y=0,z=0} = b\varepsilon_y^0$$

$$w\big|_{x=0,y=b,z=0} - w\big|_{x=0,y=0,z=0} = 0$$

$$u\big|_{x=a,y=b,z=0} - u\big|_{x=0,y=0,z=0} = a\varepsilon_x^0 + b\gamma_{xy}^0$$

$$v\big|_{x=a,y=b,z=0} - v\big|_{x=0,y=0,z=0} = b\varepsilon_y^0$$

$$w\big|_{x=a,y=b,z=0} - w\big|_{x=0,y=0,z=0} = 0$$ (66)

$$u\big|_{x=0,y=0,z=c} - u\big|_{x=0,y=0,z=0} = c\gamma_{xz}^0$$

$$v\big|_{x=0,y=0,z=c} - v\big|_{x=0,y=0,z=0} = c\gamma_{yz}^0$$

$$w\big|_{x=0,y=0,z=c} - w\big|_{x=0,y=0,z=0} = c\varepsilon_z^0$$

$$u\big|_{x=a,y=0,z=c} - u\big|_{x=0,y=0,z=0} = a\varepsilon_x^0 + c\gamma_{xz}^0$$

$$v\big|_{x=a,y=0,z=c} - v\big|_{x=0,y=0,z=0} = c\gamma_{yz}^0$$

$$w\big|_{x=a,y=0,z=c} - w\big|_{x=0,y=0,z=0} = c\varepsilon_z^0$$

$$u\big|_{x=0,y=b,z=c} - u\big|_{x=0,y=0,z=0} = b\gamma_{xy}^0 + c\gamma_{xz}^0$$

$$v\big|_{x=0,y=b,z=c} - v\big|_{x=0,y=0,z=0} = b\varepsilon_y^0 + c\gamma_{yz}^0$$

$$w\big|_{x=0,y=b,z=c} - w\big|_{x=0,y=0,z=0} = c\varepsilon_z^0$$

$$u\big|_{x=a,y=b,z=c} - u\big|_{x=0,y=0,z=0} = a\varepsilon_x^0 + b\gamma_{xy}^0 + c\gamma_{xz}^0$$

$$v\big|_{x=a,y=b,z=c} - v\big|_{x=0,y=0,z=0} = b\varepsilon_y^0 + c\gamma_{yz}^0$$

$$w\big|_{x=a,y=b,z=c} - w\big|_{x=0,y=0,z=0} = c\varepsilon_z^0.$$

In this way, one can eliminate all redundant boundary conditions. It is a shame that one has to filter out redundant ones manually if the code does not allow them. They are tedious to implement. However, this can also be done systematically if one is capable of a little programming. With Abaqus/Standard, the authors with their co-worker have developed a code called UnitCells© [20,21] which was written in Python script as a secondary development of Abaqus. A range of common unit cells have been included with relative displacement boundary conditions imposed systemically in an automated manner.

10.5 3D unit cells for various packed systems

The unit cells for face centred cubic packing and body centred cubic packing were obtained in [6], where Voronoi tessellations were employed in order to obtain their shapes systematically. They are shown in Figure 16. Each of them can be generalised to other shapes of the same topologies. For close packed hexagonal packing, unfortunately, the Voronoi cell would not make a unit cell as explained in [6]. A compromise is to use a hexagonal prism as the simplest geometry one can obtain for this packing. In this particular case, the boundary conditions will be identical to those as given in Section 10.3 if the same coordinate system is adopted, although many elements will have to be employed in the *x* direction in this case in general.

As has been pointed out, the shape of a unit cell does not dictate its behaviour. The dictating factors are the translational symmetries underlying the construction of the unit cell. Unit cells could have identical shapes, but rather different boundary conditions due to different symmetries involved and hence different structures. Naturally, the obtained effective properties are also different [10].
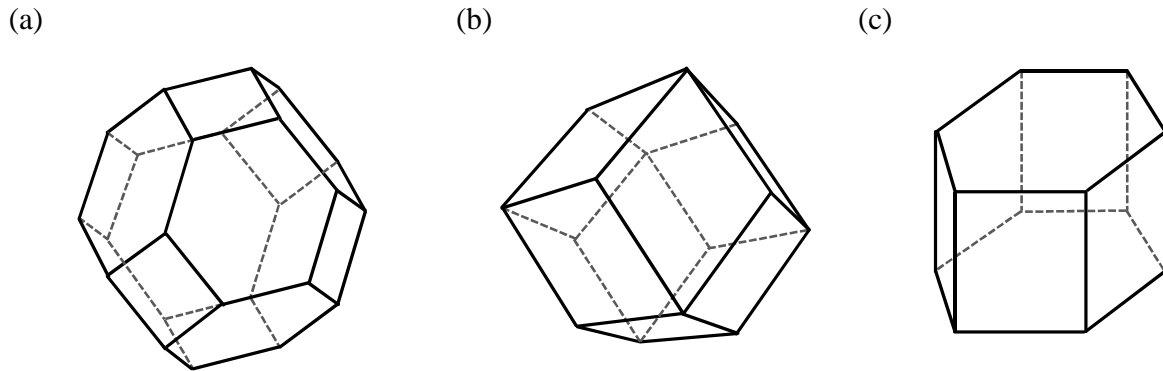
Figure 16 Unit cells for (a) body centred cubic packing (tetrakaidecahedron); (b) face centred cubic packing (rhombic dodecahedron) and (c) closed packed hexagonal packing (hexagonal prism).

For each of them, the boundary conditions can be found in [6] and will therefore not be reproduced here. Several practical issues when boundary conditions are prescribed are discussed below.

i)   All boundary conditions obtained from translational symmetries are presented in terms of relative displacements between one part of the boundary and another, associated with one of the translational symmetries. They are defined in a piecewise manner. Where those parts meet, redundant conditions are obtained at the border, which belongs to both parts. Depending on the nature of the FE code employed for the analysis, the redundant boundary conditions can sometimes cause difficulties. For instance, they cause errors and hence abort the analysis on Abaqus/Standard. In order to facilitate the analysis, one has to filter out all redundant boundary conditions. Systematic descriptions can be found in [5, 6]. However, they do not bother Abaqus/Explicit at all as explicit algorithm does not involve solving equations.

ii)   In order to impose relative displacement boundary conditions to unit cells, the parts of the boundary related through a translational symmetry should be tessellated identically. This includes the location of the nodes within each part, as well as the mesh, since identical node locations does not guarantee identical tessellation [6]. An illustration is shown in Figure 17, where the top and bottom surface share the same tessellation, while the front and back faces do not. Readers are reminded that symmetry conditions have been established based on the concept of free body diagrams, which implies the continuity between adjacent unit cells over the part of boundary they share. Continuity can only be maintained if the adjacent sides of the neighbouring unit cells are tessellated identically.

iii)   When the symmetry conditions were established in Section 5, traction conditions were obtained along with those for displacements. When applied here to formulate boundary conditions for unit cells, they are presented as relative traction and displacements between

43

different parts of the boundary of the unit cell. Throughout this section, the prescription of relative displacement boundary conditions to unit cells has been illustrated. Along with the relative displacement boundary conditions as the essential boundary conditions, the relative traction boundary conditions can be proven to be natural boundary conditions [22] according to variational calculus [9]. For finite element analyses, natural boundary conditions are approximately satisfied as the total potential energy is minimised, in the same way as equilibrium conditions are satisfied. They should not be imposed but be left alone. An example was shown in [10] where a worse approximation was obtained if the natural boundary condition was imposed.
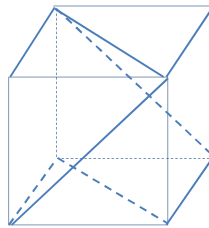

Figure 17 Compatibility of tessellations on opposite sides of a unit cell

11. Key degrees of freedom

It can be seen in the previous section that the effective strains in the upper scale are involved in the relative displacement boundary conditions. They offer some extremely useful handles for the subsequent micromechanical analysis and useful and convenient links between the two scales involved. They are not any part of the unit cell directly, but introduced into the lower scale analysis through the boundary conditions for the unit cell as extra degrees of freedom. These extra dofs can be introduced through a single node with all effective strains involved as its effective dofs. Alternatively, one can introduce extra nodes, each having one dof associated with an effective strain. They can be prescribed to the values of desirable effective strains as prescribed 'displacements'. Out of the analysis, reactions at these dofs can be obtained. It can be shown that these reaction 'forces' are associated with the effective stresses corresponding to the effective strains.

Alternatively, concentrated 'forces' can be prescribed to these extra dofs. In this way, effective stresses are prescribed. Out of the analysis, the nodal 'displacements' can be obtained at these extra dofs. They give the effective strains directly.

Each of the two approaches described above in terms of the use of the extra dofs have their convenience, depending on the outcome required. If one is interested in the stiffness matrix of the material, one can obtain a column of the stiffness matrix by prescribing a unit effective strain at a time. When all the effective strains have been exhausted, the complete stiffness matrix is

obtained. However, if one is interested in the effective elastic constants, such as Young's moduli, Poisson's ratios and shear moduli, applying uniaxial effective stress or pure shear stress will help to obtain these material properties more directly.

These extra dofs are effective strains at the upper length scale, but involved in the boundary conditions for the analysis at the lower length scale. They are therefore the key links between the two scales involved in the problem and are referred to as the key degrees of freedom (Kdofs). Their significances will be further explored in the next section.

12. Average Stresses, Average Strains and Effective Material Properties

The average stresses and strains over the unit cell as obtained from the lower length scale analysis give the effective stresses and strains in the upper length scale. Without the concept of the key degrees of freedom, one would have to average stresses and strains over the unit cell in order to find the effective stresses and strains. This is usually not a process as perceived by many as often found in the literature. These averages should not be arithmetic averages of the stresses and strains obtained at the integration points. They should be weighted by the volume of the elements and the weights associated with specific integration points. A substantial post-processing is required, which is usually outside the standard provision of most commercial FE codes. Failing to incorporate these in the calculation is certainly another possible confusion associated the use of unit cells. As an observation, very rarely, if any, the details of the procedure of finding such averages have been included in publications involving the use of unit cells. In at least some of these cases, it was probably a subject better to be kept under the carpet.

Having introduced the Kdofs, such effective stresses and strains can be obtained effortlessly as direct output from the FE analysis. The Kdofs are effective strains directly, whether they have been prescribed or obtained as the analysis outcomes. The concentrated forces at them, whether as reactions to the prescribed effective strains or as the prescribed loads, are associated with the effective stresses as follows.

$$
\begin{aligned}
F_x &= V\sigma_x^0 \\
F_y &= V\sigma_y^0 \\
F_z &= V\sigma_z^0 \\
F_{yz} &= V\tau_{yz}^0 \\
F_{xz} &= V\tau_{xz}^0 \\
F_{xy} &= V\tau_{xy}^0
\end{aligned}
, \tag{67}
$$

where V is the volume of the unit cell, or, in the case of 2D unit cells, the area of the unit cell. One might have doubt about the volume involved in the expression above. It is correct. The

45

correct dimension of these 'forces' is force time length, unlike conventional forces. The reason is that their conjugates, the Kdofs, are dimensionless, rather than conventional displacements of the dimension of length.

If these concentrated forces are prescribed at the values equal to the volume of the unit cell one after another in a series of analyses, equivalently, one is prescribing a unit stress, and the obtained effective strains can lead to effective material properties. In general, the effective properties can be evaluated from concentrated 'forces' and the 'nodal displacements' as these Kdofs as follows.

$$E_x^0 = \sigma_x^0 / \varepsilon_x^0 = F_x / V\varepsilon_x^0,$$

$$v_{xy}^0 = -\varepsilon_y^0 / \varepsilon_x^0 , \tag{68}$$

$$v_{xz}^0 = -\varepsilon_z^0 / \varepsilon_x^0 ,$$

while $\quad \sigma_y^0 = \sigma_z^0 = \tau_{yz}^0 = \tau_{xz}^0 = \tau_{xy}^0 = \Delta T = 0 \quad$ or $\quad F_y = F_z = F_{yz} = F_{zx} = F_{xy} = \Delta T = 0$;

$$E_y^0 = \sigma_y^0 / \varepsilon_y^0 = F_y / V\varepsilon_y^0,$$

$$v_{yx}^0 = -\varepsilon_x^0 / \varepsilon_y^0, \tag{69}$$

$$v_{yz}^0 = -\varepsilon_z^0 / \varepsilon_y^0,$$

while $\quad \sigma_x^0 = \sigma_z^0 = \tau_{yz}^0 = \tau_{xz}^0 = \tau_{xy}^0 = \Delta T = 0 \quad$ or $\quad F_x = F_z = F_{yz} = F_{zx} = F_{xy} = \Delta T = 0$;

$$E_z^0 = \sigma_z^0 / \varepsilon_z^0 = F_z / V\varepsilon_z^0,$$

$$v_{zx}^0 = -\varepsilon_x^0 / \varepsilon_z^0, \tag{70}$$

$$v_{zy}^0 = -\varepsilon_y^0 / \varepsilon_z^0,$$

while $\quad \sigma_x^0 = \sigma_y^0 = \tau_{yz}^0 = \tau_{xz}^0 = \tau_{xy}^0 = \Delta T = 0 \quad$ or $\quad F_x = F_y = F_{yz} = F_{zx} = F_{xy} = \Delta T = 0$;

$$G_{yz}^0 = \tau_{yz}^0 / \gamma_{yz}^0 = F_{yz} / V\gamma_{yz}^0, \tag{71}$$

while $\quad \sigma_x^0 = \sigma_y^0 = \sigma_z^0 = \tau_{xz}^0 = \tau_{xy}^0 = \Delta T = 0 \quad$ or $\quad F_x = F_y = F_z = F_{zx} = F_{xy} = \Delta T = 0$;

$$G_{zx}^0 = \tau_{zx}^0 / \gamma_{zx}^0 = F_{zx} / V\gamma_{zx}^0, \tag{72}$$

while $\quad \sigma_x^0 = \sigma_y^0 = \sigma_z^0 = \tau_{yz}^0 = \tau_{xy}^0 = \Delta T = 0 \quad$ or $\quad F_x = F_y = F_z = F_{yz} = F_{xy} = \Delta T = 0$;

$$G_{xy}^0 = \tau_{xy}^0 / \gamma_{xy}^0 = F_{xy} / V\gamma_{xy}^0 , \tag{73}$$

while $\quad \sigma_x^0 = \sigma_y^0 = \sigma_z^0 = \tau_{yz}^0 = \tau_{xz}^0 = \Delta T = 0 \quad$ or $\quad F_x = F_y = F_z = F_{yz} = F_{xz} = \Delta T = 0$;

$$\alpha_x^0 = \varepsilon_x^0 / \Delta T , \qquad \alpha_y^0 = \varepsilon_y^0 / \Delta T , \qquad \alpha_z^0 = \varepsilon_z^0 / \Delta T , \tag{74}$$

while $\quad \sigma_x^0 = \sigma_y^0 = \sigma_z^0 = \tau_{yz}^0 = \tau_{xz}^0 = \tau_{xy}^0 = 0 \quad$ or $\quad F_x = F_y = F_z = F_{yz} = F_{zx} = F_{xy} = 0$.

In the above formulae for effective properties, it is essential that each of them is applied strictly under the conditions specified. In principle, Young's moduli and Poisson's ratios should be obtained under respective uniaxial stress state and shear modulus under pure shear stress state at constant temperature and thermal expansion under a stress-free state. Any violation of the conditions will inevitably result in misinterpretation of the outcomes as the conditions are required according to the definitions of these material properties.

In the above expressions, one can observe once again the convenience of the Kdofs introduced to the formulation of unit cells. With them, effective stresses, strains and properties in the upper length scale can be obtained directly out of the lower scale modelling, serving as the most effective links between the two scales.

13. Further Symmetries within a Unit Cell

Materials of regular structures in their lower length scale often possess additional symmetries, typically, reflectional and rotational ones, in addition to translational ones which have been made extensive use of above in order to establish the unit cells and to formulate the relative displacement boundary conditions. Just like the shapes of the unit cells defined through translational symmetries lack uniqueness, the applications of further symmetries present in the unit cell obtained add a substantial variety to the subject. Without due care and systematic approach, one can easily get confused.

Before committing to any attempt along this line, readers must be made aware the following. Translational symmetry transformations do not upset the sense of loading, nor the sense of any stress and strain component. A common set of boundary conditions can be used for all loading cases. However, reflectional and rotational symmetry transformations alter the sense of loading sometimes, as well as the senses of some of the stress and strain components. As a result, one may have to impose different boundary conditions to the same unit cell obtained in order to analyse it under different loading conditions specified through the effective stresses or strains in the upper length scale.

Additional symmetries cannot be taken for granted. They depend on the selection of the shape of the unit cell out of translational symmetries alone. For instance, each of the two unit cells A and B as shown in Figure 18 makes a unit cell based on translational symmetries in horizontal and

vertical directions. Apparently, there are quite a few reflectional and rotational symmetries within A, but none in B. If one wishes to take advantages of further symmetries available in a unit cell in order to further reduce its size to be analysed, he/she needs to be mindful of such symmetries.
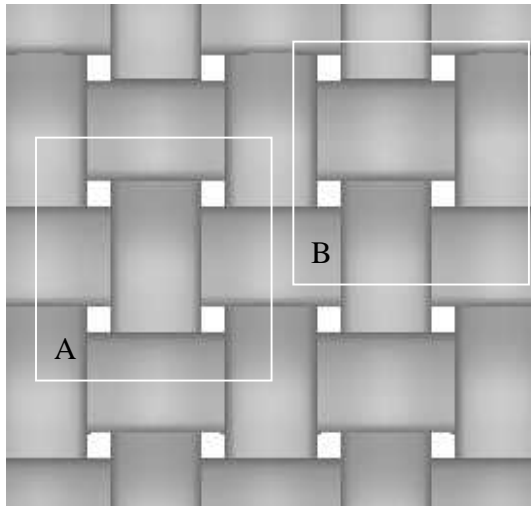

Figure 18 Examples of choices of unit cells for plain weave textile composite

As it has been pointed out previously, the shape of a unit cell does not dictate the material it represents. Under different boundary conditions derived from different symmetries, the unit cells of an identical shape can be related to different structures and hence represent different materials [10].

A typical use of additional symmetries to unit cells for hexagonally packed UD composites was elaborated in [2,4,10,23]. Employing orthogonal translational symmetries alone, a unit cell can be obtained as shown in Figure 10, which has often been employed in the literature. The benefits of it are its rectangular shape and, most importantly, the one common set of boundary conditions out of translational symmetries applies to all loading cases. Within it, the presence of reflectional symmetries about central axes in horizontal and vertical directions reduce the size to a quarter of it. Use of it can also be found in the literature but it should be regarded as the least competent application. Apart from being rectangular, there has hardly any benefit from using it. The most efficient use is to apply a further 180° rotational symmetry and one ends up with a unit cell of the size reduced to 1/8 of the original one. The down side of it is that different boundary conditions have to be imposed for different loading conditions, same as its quarter sized counterpart in this respect. Depending on the borderline chosen to partition the quarter sized unit cell using the rotational symmetry in order to obtain the 1/8 sized one, a range of unit cells of various shapes as can be found in the literature have been unified. If anything, the most significant differences between them turn out to be their friendliness to FE meshing. The actual boundary conditions can all be found in [4].

For the same problem of UD composites of hexagonal packing, if one is prepared to adapt to non-orthogonal translational symmetries, the hexagonal unit cell as shown also in Figure 14 is a nice candidate. It is half of the size as the original rectangular one as obtained from orthogonal translations alone. If one further employs the reflectional symmetries, the same unit cell would be obtained as described in the previous paragraph.

Another example is with the plain weave composite as shown in Figure 19. By using reflectional symmetries about the horizontal and vertical central axes, it can be reduced to a quarter. Further, using the rotational symmetries horizontal and vertical axes passing the centre of the quarter unit cell, the final size can be reduced to 1/16 of the original size, as shown by the red square. Again, because of the use of reflectional and rotational symmetries, different boundary conditions will have to be imposed for different loading conditions. The actual boundary conditions can be found in [23] for interested readers.
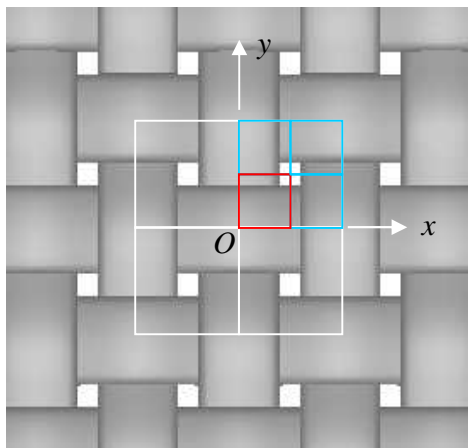

Figure 19 Plain weave and unit cell models based on the use of various symmetries

Whenever a reflectional or rotation symmetry has been used, one has to accept the consequence, i.e. boundary conditions would vary from loading case to loading case, as the price to be paid for the reduced size in the unit cell. However, there could be one compromise when a special symmetry is present, central reflection. Earlier in this chapter, it has been said that there were only three types of independent symmetries, translation, reflection and rotation. Central reflection is indeed not independent. In fact, it is a combination of a reflection and a rotation. A special feature of this is that the sense of the effective stresses and strains which defined the loading cases remain unchanged under this particular symmetry transformation. If it is available, by making use of it, the size of the unit cell can be halved while all loading cases can be analysed using a single set of boundary conditions. Interested readers are advised to consult Ref. [2].

Additional symmetries present in the structure offer the opportunity of minimising the size of the unit cell to be analysed but this comes at a price. One of the complications is the fact that some of the loading conditions associated with the shear have to be analysed under different boundary conditions, as has been mentioned already. Even worse, they bring a lot of confusion into the

49

study to such an extent that the study is some kind of myth, where certainty about boundary conditions is presumed to be irrelevant, and they had to be 'proposed', 'assumed', 'approximated' or simply just as they are without any justification, as was cited in the Introduction. An example can be shown through the construction of the UC for UD composites of hexagonal packing. Most of shaded shapes shown in Figure 20 had been employed by some researchers, in particular, the one with curved side, in addition to some more to be discussed later. They had not been unified until Ref. [4]. Orthogonal translations leads to either of the two large rectangular unit cells. Reflectional symmetries further bring them to a quarter as highlighted. The final rotational symmetry about the centre P of the quarter reduce the UC to those as shaded using various borderlines to partition the quarter UC. The requirements for the borderline is that it passes P and it is 180° rotationally symmetric about P. Special selections of this borderline have been illustrated in Figure 20 using dash-double-dot chain to reproduce all shapes cited, including the curved sided one, although absolutely no benefit whatsoever can be gained by doing so, except adding to the myth.
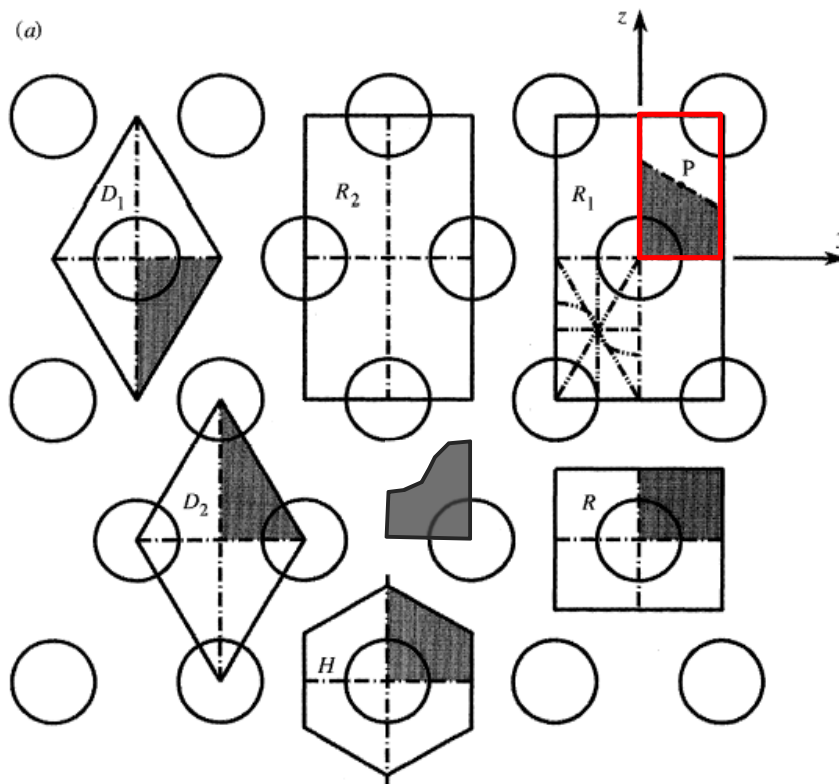

Figure 20 Various periodic elements and unit cells

In fact, the rectangular quarter sized UC as shown in Figure 21 has been the most popular one in use in the literature. In fact, the use of it exposes the user's incompetence in formulating UCs. Having employed reflectional symmetries, one has lost the simplicity of a single set of boundary

50

conditions for all loading conditions. If so, why not take a step further to half the size of it by taking advantage of the rotational symmetry about the centre as marked? Of course, the boundary conditions will be a little more complicated and hence require a slightly higher level of competence to formulate. The same can be said about the triangular UC as also shown in Figure 21, where there is still a reflectional symmetry left unused. In this particular case, had the boundary conditions been formulated correctly, those for a further reduced sized UC would not be any more complicated, if any difference, simpler. The competence required is to spot the presence of a further symmetry, before it has been pointed out, of course.
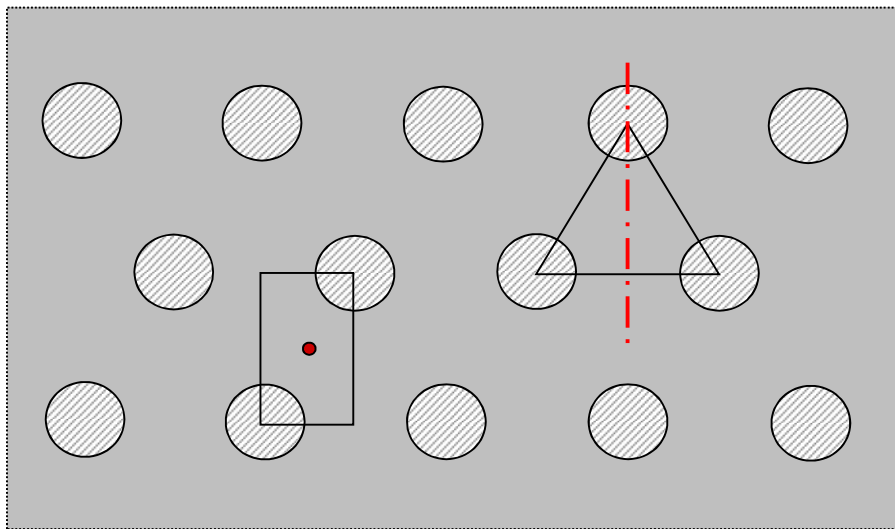

Figure 21 Shapes of unit cells which can be further simplified using available symmetries

For the particular problem of UD composite of hexagonal packing, more shapes can be found as shown in Figure 22. All of them have used only the translational symmetries and hence a single set of boundary conditions applied to all the loading conditions. The diamond-shaped and the hexagonal unit cells are exactly of the same size. The diamond-shaped involves two translational symmetries, while the hexagonal three. On the other hand, the former is partitioned into five zones, while the latter into two. This could make a bit of difference in meshing. The commonality between them is that the translations involved are non-orthogonal. As a result, in the obtained boundary conditions the average strains appear to be coupled, i.e. multiplicity of them is seen in a single equation, and the derivation of them is relatively demanding.

If one wish to trade the computational efficiency for the complications in derivation, the rectangular unit cell as also shown in Figure 22 can be used. It is twice of the size of the other two. However, because the translations involved are orthogonal and are both along the

51

coordinate axes, the obtained boundary conditions are slightly simpler. Users are reminded that a mesh of twice the size usually take much more than twice the computational time. Eight times is the norm, but slightly more conservative as an estimate.
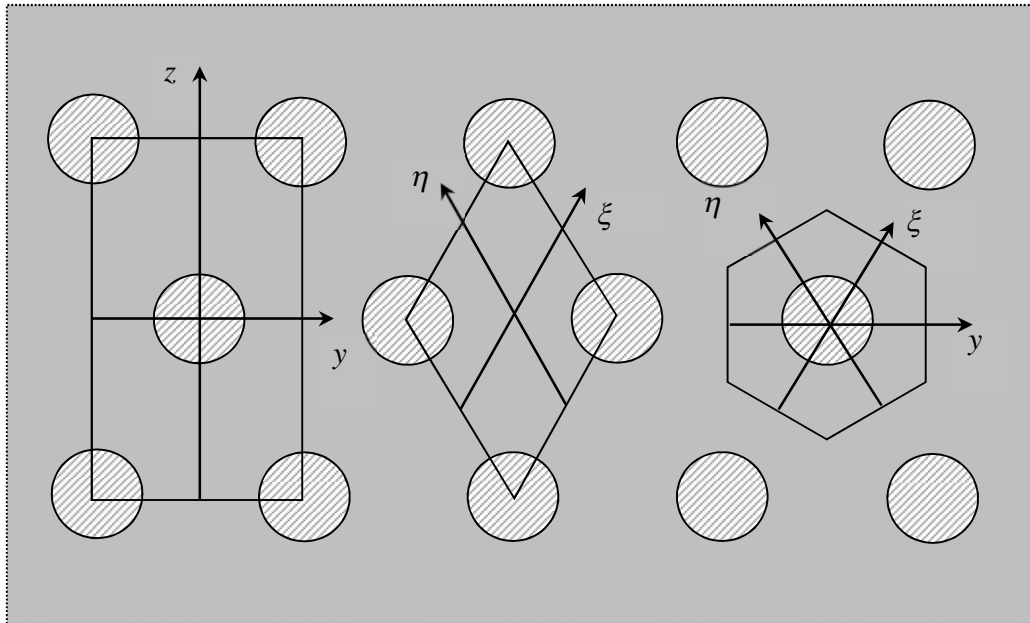

Figure 22 Unit cells for UD composites of hexagonal packing generated using translational symmetries alone

14. The Roles of Each Type of Symmetry in Material Categorisation and Characterisation

The study as presented in this chapter rests heavily on the understanding of symmetry and systematic approaches of taking advantage of them. They have been used in multiple ways. To avoid any confusion, the roles each of them plays are summarised here under the headings of material categorisation and characterisation, respectively.

14.1   Material categorisation

Translational symmetries are the basis of homogenisation of materials from their lower length scale heterogeneity to upper scale homogeneity. For materials of regular structure at lower scale, the translational symmetries can be literal. Otherwise, for materials of random structures, they will have to be justified under a statistic sense. The magnitudes of these translations define the boundary up to which materials can be assumed to be homogeneous.

Reflectional symmetries identify principal plane of the material. Materials having one principal plane are categorised as monoclinic. Materials having two principal planes perpendicular to each other are categorised as orthotropic. A third plane perpendicular to both principal plane is also a

principal plane, whether there exists or not any obvious reflectional symmetry about this plane. However, the third principal plane does not add any new feature to the material. Axes perpendicular to principal planes are principal axes.

180° rotational symmetries identify principal axis of the material. Materials having one principal axes are categorised as monoclinic. Materials having two principal axes perpendicular to each other are categorised as orthotropic. A third axes perpendicular to both principal axes is also a principal axis, whether there exists or not any obvious rotational symmetry about this axis. However, the third principal axis does not add any new feature to the material. Planes perpendicular to principal axes are principal planes.

14.2   Material characterisation

Translational symmetries are the basis of defining UCs at their lower length scale. The outcomes of the analysis of the UCs characterise the materials represented by the corresponding UCs.

Reflectional and rotational symmetries, where exist, can help to reduce the sizes of the UC as obtained from translational symmetries alone. However, this usually comes at a price, i.e. a UC needs to be analysed using different boundary conditions for different loading conditions. On the other hand, the UCs obtained from translational symmetries alone can be analysed using a single set of boundary conditions for all loading conditions.

An exception is central reflection as a combination of a reflectional symmetry and a rotational symmetry. Whilst it can halve the size of the UC to be analysed, a single set of boundary conditions will be sufficient for all loading conditions.

15. 'Sanity Checks' as Basic Verifications

The procedure of formulating unit cells as presented in previous sections of this Chapter has been systematic, but could be tedious to implement. There are many places mistakes could be easily made. Filtering out such mistakes is not straightforward. This has probably been one of the reasons for some users to follow an intuitive approach and create unit cells in a rather casual manner. They have probably been much encouraged when they could get something working fairly easily, in particular, cases involving uniaxial direct stress. However, the reliable range of one's intuition is usually limited. The trend may turn sharply once the shear is involved. This is perhaps the reason why 9 out of 10 publications in the literature shied away from shear, as if shear was irrelevant. For any serious micromechanical material characterisation, the systematic approach as presented in this chapter is the way forward. Being systematic, it can be relatively easily programmed into some fixed templates. An extreme case of such development has been demonstrated through a code developed at Nottingham, UnitCells© [20,21]. It is highly

automated with literally no need of any user's interference in setting up the boundary conditions and processing the results.

Whether the analysis is to be carried out manually or automatically, it is crucial that means are available to verify that all the measures have been implemented correctly. In this respect, unit cell users are often desperately keen to validate their results against the experimental results. However, the reality is that experimental data are always limited, and there are only limited aspects that can be examined and measured experimentally. Fitting to one aspect of the experiment can hardly be considered as validation, especially when there are obvious anomalies where the predicted results are against common sense in other aspects.

As far as the development of the micromechanical material characterisation tools is concerned, one needs verifications more than the experimental validations. There are a number of 'sanity checks' as will be described in detail below. If any unit cell formulated and implemented fails to pass any of the 'sanity checks', it is incorrect, no matter how well some of the results agree with experimental data.

The first set of 'sanity checks' can be set up as follows. A single set of material properties are is assigned to all phases of the constituents involved in the unit cell, so that the unit cell would essentially represent a homogeneous and isotropic material. The analyses are carried out under all loading conditions. In each case, perfectly uniform stress and strain fields should be obtained for each loading case. Otherwise, the unit cell has not been either formulated or implemented correctly. When stress contours are plotted in this case, multi-coloured images indicate fault, as correct stress distributions must be uniform and hence uni-coloured. Typical stress concentrations are found around the vertices which signify the incorrect boundary conditions in most cases.

Having achieved uniform stress and strain field, a check on their values is simple and essential, as they must correspond to the prescribed loading identically. The stresses and strains should be related according to the material properties as assumed for these analyses. One also needs to check the ratios between the strains, as they should coincide with the Poisson's ratios as assigned to the material to facilitate the analyses.

Finally, the data processing phase of the analyses should be conducted. The predicted effective properties must be identical to those assigned to the material to facilitate the analyses.

Having passed the 'sanity checks' as proposed above, one must have eliminated 90% of the errors made in the implementation of a unit cell one way or another. One probably finds at least 90% of efforts to implement a unit cell would have been consumed in order to pass these checks. Without offending users, one would probably find 90% of the unit cells as presented in the literature would not have been able to pass these 'sanity checks' in one respect or another. Of course, most of them did not have the boundary conditions employed shown in the sources where they were published, as if boundary conditions were irrelevant or obvious.

16. UD Composites and Transverse Isotropy

Unidirectionally fibre reinforced composites (UD) are the most common type of composites. They can constitute individual plies in laminated structures or tows in textile composites. Their characterisation is one of the most popular and fundamental exercises in micromechanical analysis. Fibres in a UD composite are usually distributed at random over its cross section perpendicular to the fibres. Their statistical uniformity often serves as the basis for idealisations, in which fibres are assumed to be packed in a regular pattern, typically, square packing and hexagonal packing. Unit cells can then be constructed as shown in previous sections. They have been adopted in most cases without much justification in terms of their representativeness. Often, experimental data were brought in too swiftly as the ultimate authoritarian measure. One aspect often being overlooked is the transverse isotropy.

A square packing as an idealisation of UD composites does not preserve transverse isotropy. Excellent comparison with the experimental data, e.g. transverse Young's modulus E_2, obtained in one direction, has automatically guaranteed a bad comparison if the value was obtained in a different direction, e.g. 45° between axes y and z [5]. On the other hand, a hexagonal packing preserves the transverse isotropy.

17. RVE for Randomly Distributed Inclusions

In Section 8, the falsification of periodicity for random structures was dismissed. However, there still remains a question as to how an untampered RVE should be analysed. Without geometric periodicity, it is no longer possible to obtain the precise boundary conditions for the RVE to be analysed, whether in terms of displacements or traction. Inside a large/infinite medium, before the solution to the problem has been found, it is impossible to identify a path along which either displacements or traction would be constant to enable the definition of the path as a part of the boundary of the RVE. Along the boundary of an RVE, no matter how the displacements or the traction is prescribed, significant errors will be introduced. However, in [16], it was shown that such errors are only of local effects. Several characteristic lengths away from the boundary, the errors tend to diminish. The characteristic length can usually be defined in terms of the dimensions of the inclusions or the average spacing between them. This was not by coincidence. The underlying rule is the St. Venant principle. Guided by this, an approach can be readily put forward.

The methodology of formulating an appropriate RVE for micromechanical analysis is as follows. Assuming that the smallest RVE has been identified, it is defined as the inner zone. Next, an extended zone is introduced around it, with the sides which are several characteristic lengths beyond the sides of the inner zone, as illustrated in Figure 23. The extended zone is also an RVE

by definition. Both RVEs should at least share the volume fraction with the material as a whole. The extended RVE is analysed by applying constant displacements to the boundary according to the desirable loading conditions, and the solution can be found, which is known to be erroneous. However, errors are meant to be found only around the boundary of the extended zone. Within the inner zone, which is the smallest RVE, sufficiently accurate solution can be obtained. It is easy to envisage that the boundary of the inner RVE does not deform into any regular shape after the deformation, in general. If the average stresses and strains are found from the inner zone, effective material properties can be worked out. They are free from the effects of erroneous boundary conditions. Thus, no tampering is required and the randomness of the structure has not been compromised in any way. More examples of applications of the methodology can be found in [24,25,26].
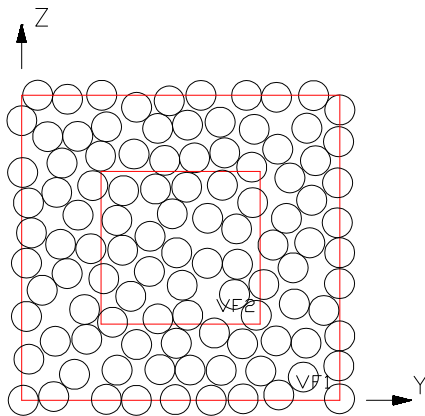

Figure 23 RVE for a UD composite with random fibre distribution over its transverse cross section

In addition to the extended size of the RVE to be analysed as the price to pay, another increased the demand is in the post-processing. The average stresses and strains will have to be found. This will have to involve assigning correct weight to the stresses and strain obtained at each integration point.

Another observation made in [16] was that prescribing constant traction to the boundary of the larger RVE tended to result in greater errors and therefore it takes longer distance for the errors to diminish than prescribing constant displacement.

18. Applications to Textile Composites

Textile composites are particularly relevant to the theoretical development as presented in this chapter due to their regular and periodic structures at a mesoscale. The considerations as given to symmetries are particularly useful. Given their regularity in the fibre tow interlacing

structures, macroscale homogeneity can be easily justified based on the presence of translational symmetries. However, the homogeneity is an acceptable assumption only at a macroscale, i.e. at a characteristic dimension orders of magnitude larger than the periods in the meso-structure.

Textile composites are typical multiscale materials. Under the visible features is a micro-structure at mesoscale, where UD fibres are bonded together into fibre tows. Micromechanics can be employed to characterise the tow material as a UD composite, where use can be made of the unit cells as presented in Section 10.1 and 10.3 for this purpose.

The microscale to mesoscale homogenisation is straightforward as the relevant unit cells to facilitate the process have been presented in Section 10. Discussion below will be made on homogenisation from the mesoscale to the macroscale only.

18.1   Reflectional and rotational symmetries for material categorisation

Textile composites made of simple woven preforms, such as plain weaves as shown in Figure 18, can be easily categorised into the orthotropic family due to the apparent presence of planes of reflectional symmetries. However, reflectional symmetries are not always available, whilst rotational symmetries are sometimes present.

In particular, there is not a single reflectional symmetry in a 3D 4-axial braid, as shown in Figure 24, which is a typical form of reinforcement in 3D braided composites [27]. 3D braiding offers superb integrity and it allows the cross-section to vary relatively easily. The structure of the braid is such that there are rotational symmetries about 3 perpendicular axes, x, y and z, as shown in Figure 24 and, as a result, 3D 4-axial braided composites are orthotropic. The principal axes of orthotropy are the axes of rotational symmetries, which do not usually coincide with the direction of any fibre tows.

Figure 24 Unit cell of four-axial 3D braided composite

Another example is twill weave composites, see Figure 25. Twill weaves are usually much easier to drape to conform to curved shapes than plain weaves, and hence they have significant potential in applications. Again, in a typical twill weave, no reflectional symmetry is available, while rotational symmetries are present [13]. The in-plane principal axis identified by the rotational symmetry in a twill weave composite is inclined at 45° to the direction of fibre tows. It is also rotationally symmetric about an axis out of the plane of the weave, identifying another principal axis. The material is therefore orthotropic although none of the principal axes of the orthotropy coincides with the directions of fibre tows. The third principal axis, being perpendicular to the two identified through rotational symmetries, is inclined at the other 45° to the direction to the fibre tows. It is worth noting that there is no obvious symmetry of any kind, either rotation about the third principal axis, or reflection about the plane perpendicular to the third principal axis.
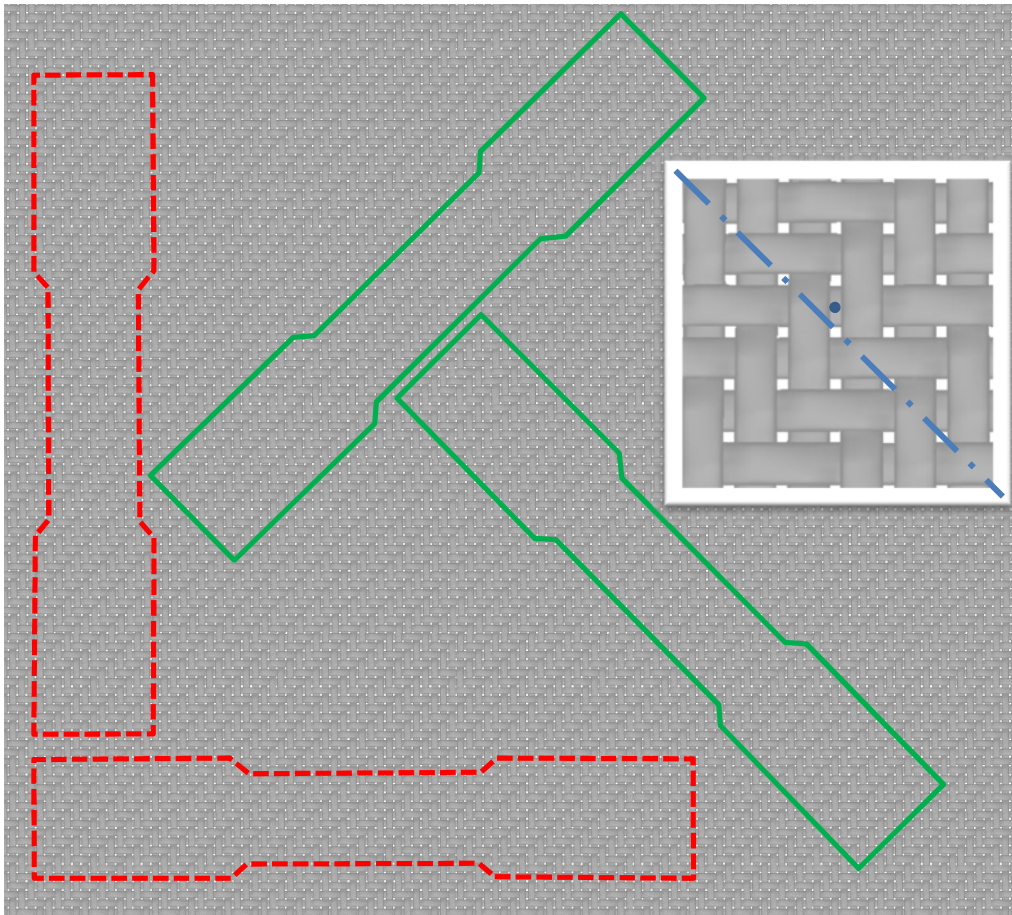

Figure 25 Twill weave, its principal axes resulting from rotational symmetries (inset: the diagonal axis and the axis out of the plane represented by the dot), correct directions for material characterisation (green), their misperception (red)

Readers are reminded that there is no available industrial standard applicable to generally anisotropic materials. Existing standards requires the materials to be tested to fall in the category of orthotropy. Applying the standards blindly amounts to abuse of them and the consequences could be serious. Without appropriate emphasis, the pre-conditions of these standards could be easily overlooked. There is perhaps no lack of examples where twill weave composites are being characterised directly in the fibre tow directions in the plane of the twill weave. This is the reason for advocating material categorisation as an essential step before material characterisation. Whilst it could sound like stating the obvious, obvious rules are there to observe, not to ignore. The authors are taking this opportunity to make a serious call as a first attempt to the best of their knowledge for future practices in this field: categorise a material before its characterisation!

18.2   Unit cells

Having categorised a textile composite, an appropriate unit cell can be formulated, first of all based on the translational symmetries present in the meso-structure. The sizes of such unit cells can often be significantly reduced by taking advantage of additional reflectional and/or rotational symmetries present in the meso-structure. Two examples are shown below.

18.2.1 Plain weave composites

The plain weave unit cell obtained through translational symmetries alone can be seen in Figure 26(a). The boundary conditions obtained in Section 10.4 for the rectangular parallelepiped can be readily applied to it.

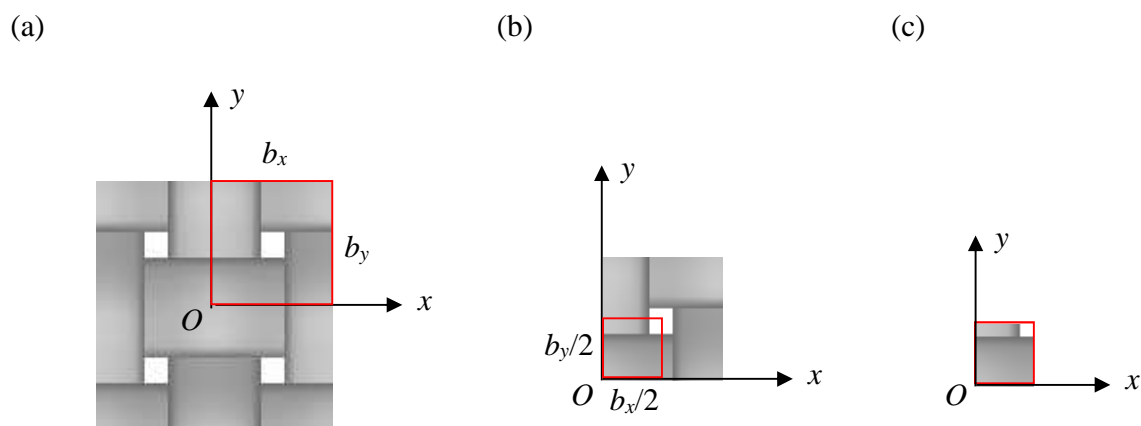(a)   (b)   (c)

Figure 26 Unit cells for plain weave based on the use of various symmetries: (a) Full sized UC based on translational symmetries alone, (b) Quarter sized UC after the use of reflectional symmetries, and (c) 1/8 sized UC after further use of 180 degrees rotational symmetries

As was mentioned in Section 13, there exist two reflectional symmetries about the horizontal and vertical axes. Using them, the size of the unit cell can be reduced to 1/4 of its original size. However, there is not much benefit to stay at this point. In this quarter sized unit cell, there are two more rotational symmetries about the horizontal and vertical axes passing through the centre of it. Making use of them, the size of the unit cell can be further reduced to 1/16 of the original size. Having used the reflectional and rotational symmetries, boundary conditions are different for different loading conditions. They are summarised as follows, while the detailed derivation can be found in [23].

Under $\sigma_x^0, \sigma_y^0, \sigma_z^0$ or any combination of them:

$$u' - u = 0$$
$$v' + v = b_y \varepsilon_y^0 \qquad \text{on } y = b_y/2, \tag{75a}$$
$$w' + w = 0$$

$$v = \frac{1}{2} b_y \varepsilon_y^0 \qquad \text{at } y = b_y/2 \ \& \ z = 0, \tag{75b}$$
$$w = 0$$

$$u' + u = b_x \varepsilon_x^0$$
$$v' - v = 0 \qquad \text{on } x = b_x/2, \tag{75c}$$
$$w' + w = 0$$

$$u = \frac{1}{2} b_x \varepsilon_x^0 \qquad \text{at } x = b_x/2 \ \& \ z = 0. \tag{75d}$$
$$w = 0$$

Under τ_{yz}^0:

$$u' - u = 0$$
$$v' + v = 0 \qquad \text{on } y = b_y/2, \tag{76a}$$
$$w' + w = 0$$

$$v = 0$$
$$\qquad \text{at } y = b_y/2 \ \& \ z = 0, \tag{76b}$$
$$w = 0$$

$$u' - u = 0$$
$$v' + v = 0 \qquad \text{on } x = b_x/2, \tag{76c}$$
$$w' - w = 0$$

$$v = 0 \qquad \text{at } x = b_x/2 \ \& \ z = 0. \tag{76d}$$

Under τ_{xz}^0:

$$u' + u = 0$$
$$v' - v = 0 \qquad\qquad \text{on } y=b_y/2, \qquad\qquad\qquad (77a)$$
$$w' - w = 0$$

$$u = u_C \qquad\qquad \text{at } y=b_y/2 \ \& \ z=0, \qquad\qquad (77b)$$

$$u' + u_P = 0$$
$$v' - v_P = 0 \qquad\qquad \text{on } x=b_x/2, \qquad\qquad\qquad (77c)$$
$$w' + w_P = 0$$

$$u = 0$$
$$w = 0 \qquad\qquad \text{at } x=b_x/2 \ \& \ z=0. \qquad\qquad (77d)$$

Under τ_{xy}^0:

$$u' + u = b_y \gamma_{xy}^0$$
$$v' - v = 0 \qquad\qquad \text{on } y=b_y/2, \qquad\qquad\qquad (78a)$$
$$w' - w = 0$$

$$u = \frac{1}{2} b_y \gamma_{xy}^0 \qquad\qquad \text{at } y=b_y/2 \ \& \ z=0, \qquad\qquad (78b)$$

$$u' - u = 0$$
$$v' + v = 0 \qquad\qquad \text{on } x=b_x/2, \qquad\qquad\qquad (78c)$$
$$w' - w = 0$$

$$v = 0 \qquad\qquad \text{at } x=b_x/2 \ \& \ z=0. \qquad\qquad (78d)$$

To impose boundary conditions as given by (75)-(78), the mesh for the unit cell must be so generated that each of the two sides, $y=b_y/2$ and $x=b_x/2$, must be partitioned by plane $z=0$, i.e. each side being split into two faces. The tessellations on each pair of the faces on both sides of $z=0$ plane must be identical under the corresponding symmetries. Effectively, as far as geometric symmetries between the corresponding faces are concerned, the rotational symmetries for faces at $y=b_y/2$ and $x=b_x/2$ on opposite sides of $z=0$, as well as the translational symmetry for the top and bottom surfaces, share the same characteristics as the reflectional symmetry about $z=0$.

Apparently, each edge is shared by two faces of the unit cell. Redundant constraints arise if the conditions for each of the two faces are imposed to the same edge individually. Any redundant boundary condition can be eliminated. As it is a tedious process, it could be a rather confusing

step. The principle however is simple. Since an edge is shared by two faces, the boundary conditions on both intersecting faces apply to the edge. What one needs to do is to take the logical sum of the available conditions from both faces at the edge concerned. Detailed derivations will not be presented here, but interested readers are referred to [23] for full information.

18.2.2 3D 4-axial braided composites

Geometric periodicity is an obvious feature in the meso-structures of 3D braided fabrics and composites formed from them. The geometric symmetries associated with periodicity are translations. Using translational symmetries alone, a unit cell as sketched in Figure 27(a) can be defined, which will be referred to as *full-size unit cell*. In Figure 27, the blobs on various edges are truncated segments of tows.

Within the full-size unit cell, other symmetries are also present. Specifically, 180° rotations about all three coordinate axes are present, but only two of them are independent. Without losing generality, using the rotation about the *z*-axis, size of the unit cell can be reduced to a half, referred to as *half-size unit cell*, as shown in Figure 27(b). Another rotation about the *x*-axis can bring the size of the unit cell a quarter of the full-size unit cell, as shown in Figure 27(c), referred to as the *quarter-size unit cell*. Although this unit cell has been an apparent choice geometrically [27], it is not an optimum one as there is another useful symmetry unexploited.

Within the quarter-size unit cell, there is a further obvious symmetry. It is 180° rotation about axis y_1, which is parallel to the *y*-axis and passes through the centre of the quarter-size unit cell, as depicted in the Figure 27(c). By employing this symmetry, the size of the unit cell can be further halved, as shown in Figure 27(d), into one eighth of the full-size unit cell, referred to as *1/8 unit cell*.
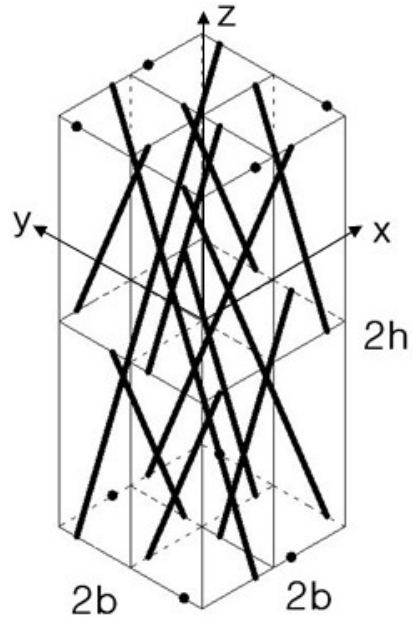
The boundary conditions have been derived systematically in [28]. Extracted from it, after constraining the rigid body translations of the UC by fixing the origin O from any displacements, the boundary conditions for the unit cell of significantly reduced size as in Figure 27(d) can be presented as follows.

Under σ_x^0, σ_y^0, σ_z^0 or any combination of them:

$$
\begin{aligned}
u + u' &= b\varepsilon_x^0 \\
v - v' &= 0 \\
w + w' &= h\varepsilon_z^0
\end{aligned}
\qquad \text{Face } z=h/2: \quad
\begin{aligned}
0 &\leq x \leq b/2 \\
-b &\leq y \leq b
\end{aligned}
\qquad (79)
$$

$$
\begin{aligned}
u\big|_{(x,y,0)} - u\big|_{(x,-y,0)} &= 0 \\
v\big|_{(x,y,0)} + v\big|_{(x,-y,0)} &= 0 \\
w\big|_{(x,y,0)} + w\big|_{(x,-y,0)} &= 0
\end{aligned}
\qquad \text{Face } z=0: \quad
\begin{aligned}
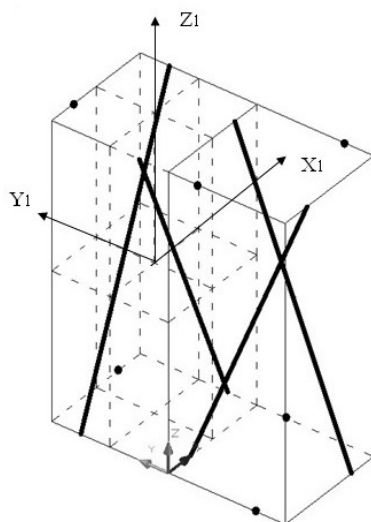0 &\leq x \leq b \\
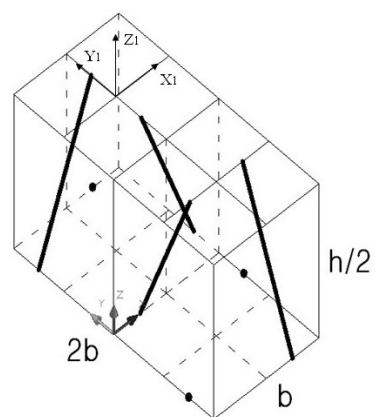-b &\leq y \leq b
\end{aligned}
\qquad (80)
$$

Figure 27 Unit cells for 3D 4-axial braided composite based on the use of rotational symmetries: (a) full size unit cell; (b) half size unit cell; (c) quarter size unit cell; (d) 1/8 unit cell.

$$u|_{(x,b,z)} - u|_{(x,-b,z)} = 0$$
$$v|_{(x,b,z)} - v|_{(x,-b,z)} = 2b\varepsilon_y^0 \qquad \text{Faces } y=\pm b: \qquad \begin{array}{l} 0 \le x \le b \\ 0 \le z \le h/2 \end{array} \qquad (81)$$
$$w|_{(x,b,z)} - w|_{(x,-b,z)} = 0$$

$$u|_{(0,y,z)} + u|_{(0,-y,z)} = 0$$
$$v|_{(0,y,z)} + v|_{(0,-y,z)} = 0 \qquad \text{Faces } x=0: \qquad \begin{array}{l} 0 \le y \le b \\ 0 \le z \le h/2 \end{array} \qquad (82)$$
$$w|_{(0,y,z)} - w|_{(0,-y,z)} = 0$$

$$u|_{(b,y,z)} + u|_{(b,-y,z)} = 2b\varepsilon_x^0$$
$$v|_{(b,y,z)} + v|_{(b,-y,z)} = 0 \qquad \text{Faces } x=b: \qquad \begin{array}{l} 0 \le y \le b \\ 0 \le z \le h/2 \end{array} \qquad (83)$$
$$w|_{(b,y,z)} - w|_{(b,-y,z)} = 0$$

Under τ_{yz}^0:

$$u|_{(x,y,h/2)} - u|_{(b-x,y,h/2)} = 0$$
$$v|_{(x,y,h/2)} + v|_{(b-x,y,h/2)} = h\gamma_{yz}^0 \qquad \text{Face } z=h/2: \qquad \begin{array}{l} 0 \le x \le b/2 \\ 0 \le y \le b \end{array} \qquad (84)$$
$$w|_{(x,y,h/2)} - w|_{(b-x,y,h/2)} = 0$$

$$u|_{(x,y,0)} - u|_{(x,-y,0)} = 0$$
$$v|_{(x,y,0)} + v|_{(x,-y,0)} = 0 \qquad \text{Face } z=0: \qquad \begin{array}{l} 0 \le x \le b \\ 0 \le y \le b \end{array} \qquad (85)$$
$$w|_{(x,y,0)} + w|_{(x,-y,0)} = 0$$

$$u|_{(x,b,z)} - u|_{(x,-b,z)} = 0$$
$$v|_{(x,b,z)} - v|_{(x,-b,z)} = 0 \qquad \text{Faces } y=\pm b: \qquad \begin{array}{l} 0 \le x \le b \\ 0 \le z \le h/2 \end{array} \qquad (86)$$
$$w|_{(x,b,z)} - w|_{(x,-b,z)} = 0$$

$$u|_{(0,y,z)} - u|_{(0,-y,z)} = 0$$
$$v|_{(0,y,z)} - v|_{(0,-y,z)} = 0 \qquad \text{Faces } x=0: \qquad \begin{array}{l} 0 \le y \le b \\ 0 \le z \le h/2 \end{array} \qquad (87)$$
$$w|_{(0,y,z)} + w|_{(0,-y,z)} = 0$$

$$u|_{(b,y,z)} - u|_{(b,-y,z)} = 0$$
$$v|_{(b,y,z)} - v|_{(b,-y,z)} = 0 \qquad \text{Faces } x=b: \qquad \begin{array}{l} 0 \le y \le b \\ 0 \le z \le h/2 \end{array} \qquad (88)$$
$$w|_{(b,y,z)} + w|_{(b,-y,z)} = 0$$

Under τ_{xz}^0:

$$u|_{(x,y,h/2)} + u|_{(b-x,y,h/2)} = h\gamma_{xz}^0$$
$$v|_{(x,y,h/2)} - v|_{(b-x,y,h/2)} = 0$$
$$w|_{(x,y,h/2)} + w|_{(b-x,y,h/2)} = 0$$

Face $z=h/2$: $\quad 0 \le x \le b/2$
$\qquad\qquad\quad -b \le y \le b$ (89)

$$u|_{(x,y,0)} + u|_{(x,-y,0)} = 0$$
$$v|_{(x,y,0)} - v|_{(x,-y,0)} = 0$$
$$w|_{(x,y,0)} - w|_{(x,-y,0)} = 0$$

Face $z=0$: $\quad 0 \le x \le b$
$\qquad\qquad\quad 0 \le y \le b$ (90)

$$u|_{(x,b,z)} - u|_{(x,-b,z)} = 0$$
$$v|_{(x,b,z)} - v|_{(x,-b,z)} = 0$$
$$w|_{(x,b,z)} - w|_{(x,-b,z)} = 0$$

Faces $y=\pm b$: $\quad 0 \le x \le b$
$\qquad\qquad\qquad 0 \le z \le h/2$ (91)

$$u|_{(0,y,z)} - u|_{(0,-y,z)} = 0$$
$$v|_{(0,y,z)} - v|_{(0,-y,z)} = 0$$
$$w|_{(0,y,z)} + w|_{(0,-y,z)} = 0$$

Faces $x=0$: $\quad 0 \le y \le b$
$\qquad\qquad\quad 0 \le z \le h/2$ (92)

$$u|_{(b,y,z)} - u|_{(b,-y,z)} = 0$$
$$v|_{(b,y,z)} - v|_{(b,-y,z)} = 0$$
$$w|_{(b,y,z)} + w|_{(b,-y,z)} = 0$$

Faces $x=b$: $\quad 0 \le y \le b$
$\qquad\qquad\quad 0 \le z \le h/2$ (93)

Under τ_{xy}^0:

$$u|_{(x,y,h/2)} - u|_{(b-x,y,h/2)} = 0$$
$$v|_{(x,y,h/2)} + v|_{(b-x,y,h/2)} = 0$$
$$w|_{(x,y,h/2)} - w|_{(b-x,y,h/2)} = 0$$

Face $z=h/2$: $\quad 0 \le x \le b/2$
$\qquad\qquad\qquad -b \le y \le b$ (94)

$$u|_{(x,y,0)} + u|_{(x,-y,0)} = 0$$
$$v|_{(x,y,0)} - v|_{(x,-y,0)} = 0$$
$$w|_{(x,y,0)} - w|_{(x,-y,0)} = 0.$$

Face $z=0$: $\quad 0 \le x \le b$
$\qquad\qquad\quad 0 \le y \le b$ (95)

$$u|_{(x,b,z)} - u|_{(x,-b,z)} = 2b\gamma_{xy}^0$$
$$v|_{(x,b,z)} - v|_{(x,-b,z)} = 0$$
$$w|_{(x,b,z)} - w|_{(x,-b,z)} = 0$$

Faces $y=\pm b$: $\quad 0 \le x \le b$
$\qquad\qquad\qquad 0 \le z \le h/2$ (96)

$$u\big|_{(0,y,z)} + u\big|_{(0,-y,z)} = 0$$
$$v\big|_{(0,y,z)} + v\big|_{(0,-y,z)} = 0 \qquad \text{Faces } x{=}0: \qquad \begin{array}{l} 0 \le y \le b \\ 0 \le z \le h/2 \end{array} \qquad (97)$$
$$w\big|_{(0,y,z)} - w\big|_{(0,-y,z)} = 0$$

$$u\big|_{(b,y,z)} + u\big|_{(b,-y,z)} = 0$$
$$v\big|_{(b,y,z)} + v\big|_{(b,-y,z)} = 0 \qquad \text{Faces } x{=}b: \qquad \begin{array}{l} 0 \le y \le b \\ -b \le z \le b \end{array} \qquad (98)$$
$$w\big|_{(b,y,z)} - w\big|_{(b,-y,z)} = 0$$

The unit cell obtained in this section is of 1/8 of the full-size unit cell, but it remains applicable for characterising the composite fully. However, macroscopic direct stresses and each macroscopic shear stress will have to be treated separately as the boundary conditions are different for each case.

The implementation of the boundary conditions presented above will require the mesh of the unit cell so created that opposite faces $y{=}\pm b$ are tessellated in exactly the same form, while faces $x{=}0$ and $x{=}b$ show symmetry about their respective centrelines parallel to the z-axis, and face $z{=}0$ and $z{=}h$ about their respective centrelines parallel to the x-axis. Similar to the full-size unit cell, redundant conditions arise at edges and vertices of the unit cell, as well as along the centreline on the x-faces. Sufficient guidance can be found in Section 10 as well as in [5, 6] if they need to be eliminated and the underlying considerations remain the same, although the symmetries involved are slightly different.

18.3   3D weaves

The use of 3D weaves as preforms for composites is attracting more and more attention in engineering. The most common types are the interlocking weave fabric as shown in Figure 28 and the non-crimp fabrics (NCFs) which will not be addressed here. The former employs straight fibre tows to form the main part of the fabric, which are bound together using a limited amount of interlacing tows. In the latter, fibre tows are placed either as the warp or the weft. While weft tows remain straight, the warp tows interlace the weft tows in a range of designed manners resulting in various fabrics, such as angle interlock, layer to layer interlock, etc.

One may find the cuboidal unit cells to be applicable to most of such 3D woven composites. The only significant extra consideration is that the textures of these weaves on the surface of the fabrics tend to be noticeably different from those in the core of the fabric. If the surface layers constitute a relatively small part of the fabric, the differences they make may be considered insignificant, hence the presence of surface layers can be neglected. Otherwise, they need to be taken into proper account.

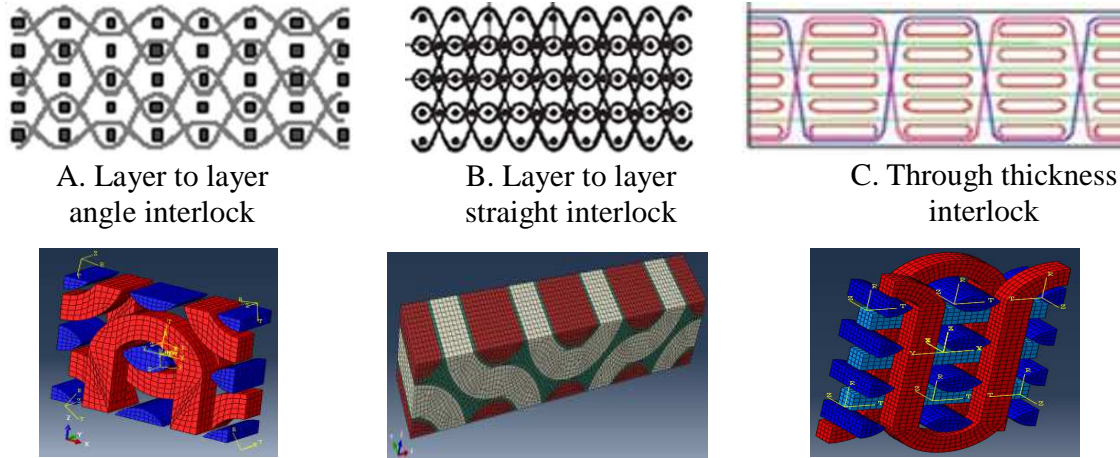| A. Layer to layer angle interlock | B. Layer to layer straight interlock | C. Through thickness interlock |

Figure 28 The most common types of 3D woven reinforcements: (a) Layer to layer angle interlock, (b) Layer to layer straight interlock, and (c) Through thickness interlock

When the full thickness is included in a UC, one may have to make a decision whether the through-thickness properties are desirable. If not, the top and bottom surfaces should be left free. Otherwise, an appropriate loading mechanism will have to be introduced. However, development of such a mechanism is beyond the scope of the present chapter.

19. Diffusion Problems

There is a large class of physical problems, including heat/electricity conduction, fluid permeability in porous medium, etc., that can be classified into the mathematical problem of diffusion, as has been addressed in [29,30,31,32]. The constitutive relationship for the diffusion problem is defined by the diffusion coefficient matrix $[k]$, which couples the field (e.g. temperature) gradient, ∇T, with the flux (e.g. heat), $\{q\}$.

$$\begin{Bmatrix} q_x \\ q_y \\ q_z \end{Bmatrix} = -\begin{bmatrix} k_{11} & k_{12} & k_{13} \\ k_{12} & k_{22} & k_{23} \\ k_{13} & k_{23} & k_{33} \end{bmatrix} \nabla T , \qquad \text{where} \quad \nabla T = \begin{Bmatrix} \dfrac{\partial T}{\partial x} \\ \dfrac{\partial T}{\partial y} \\ \dfrac{\partial T}{\partial z} \end{Bmatrix} . \tag{99}$$

All arguments made before are readily interpreted to offer necessary means to facilitate the multiscale material characterisation of this class of problems. The relative field can be given as

$$T' - T = T_x^0 \Delta x + T_y^0 \Delta y + T_z^0 \Delta z \quad , \tag{100}$$

where $\nabla T^0 = \begin{Bmatrix} T_x^0 \\ T_y^0 \\ T_z^0 \end{Bmatrix}$ is the effective field gradient in the upper length scale, and the constants Δx,

Δy and Δz are periods in x, y, and z directions, respectively, associated with the translational symmetries available in the structure in the lower length scale, although the translations do not have to be in the same directions as the coordinate axes. Boundary conditions for the unit cell can be obtained from (100) in a straightforward manner.

If any substantial difference from their mechanical counterpart, there are fewer material constants to be determined and the categorisation of anisotropy is slightly simpler, as the cubic symmetry implies isotropy.

The concepts of RVE and unit cells and their implementations are directly extended from the mechanical problem to the diffusion problem.

20. Boundary of Applicability of RVEs and UCs

Having been established as in previous sections, the RVEs and UCs, if applied appropriately, can offer an effective tool for material characterisation. However, correct formulation does not necessarily guarantee appropriate application. Coming with the formulation are the limitations on their range of applicability. The assumptions introduced in their formulation have provided good indications about such limits.

The length scale at which homogeneity can be assumed is one of the important measures. The dimensions of an RVE or UC, whilst remaining representative, should be significantly smaller than the characteristic features in its upper length scale for the uniform stress and strain field in the upper scale to be valid.

The homogeneity also places a restriction on the extent of deformation. As it is based on the regularity, in either statistical or geometric sense, any deformation violating the regularity, e.g. when deformation starts to localise, resulting in necking, discrete cracks and any other signs of material softening, is deemed to be beyond the applicability of the UCs and RVEs. There is probably no lack of examples of such abuses in the literature.

The magnitude of deformation places another restriction to the applicability of RVEs and UCs. The deformation kinematics underlying the formulation of RVEs and UCs are based on the assumption of small deformation, although blind application of the RVEs and UCs beyond the range of small deformation might be found in the literature. However, the effects of finite geometric deformation have to be taken into account when finite deformation is involved. Then

68

there will be nonlinear terms in the deformation kinematic equation. The relative displacement field will no longer be related to the effective strains in a form as simple as in (32). This in turn defines the applicability of RVEs and UCs in terms of the magnitude of deformation involved.

21. Concluding Statement

Traditionally, material characterisation has been associated with material testing to obtain desired material properties. The establishment of RVEs and UCs is to facilitate a computational means as an alternative to the physical testing, as is often referred to virtual testing. While virtual testing has never been introduced to replace physical testing completely, and it will never do, it can help to minimise the demand on physical testing, which is usually expensive and time-consuming. In many of the modern materials, in particular, in fibre reinforced composites, heterogeneity and anisotropy are often the key features. Appropriate categorisation of such materials in terms of the degree of heterogeneity and anisotropy is an essential step before their characterisation becomes meaningful. Readers are reminded that available industrial standards only support characterisation of materials in a limited category, e.g. orthotropic materials. Without appropriate categorisation, these standards could be abused, e.g. the specimens would not be loaded in their principal directions. It is important to note that the virtual testing can go beyond such limitation, although one would have to worry about its validation.

A crucial aspect underlying the applicability of RVEs and UCs is the homogeneity of the material concerned at a certain length scale. Appropriate application of them offers an effective means to homogenise the material from its lower length scale, where heterogeneity is observed in terms of the different phases as the constituents of the material. The analysis associated with them is multiscale modelling in nature, *viz.*, the analysis is conducted at a lower length scale in order to deliver effective material properties at the upper length scale, where homogeneity can be assumed. Associated length scales are therefore a crucial measure of the applicability of the analysis.

For materials of random structures at the lower length scale, homogeneity can only be justified in a statistical sense. RVEs are the appropriate means to characterise such materials. However, it should be noted that RVEs can only be representative only if they are (a) large enough in size and (b) free from artificial manipulations. A systematic approach has been represented in the Section 17 of this chapter.

In presence of symmetries in materials of regular structure at the lower length scale, use can be made of them to establish UCs to drastically reduce the demand on the material characterisation by the virtual testing means. In this respect, translations are the most important type of symmetries. Identifying their geometric presence is a relatively easy step. Interpreting their implications on the UC to be formulated, in particular, the derivation of precise boundary conditions for the analysis of the UC, requires a new concept, i.e. the relative displacement field.

With it, the formulation of the UC will then rest on a firm ground, whilst most mistakes found in the field were due to the lack of this concept as a starting point. Further reflectional and rotational symmetries, if present in the UC identified, can be taken advantage of to reduce the size of the UC to be analysed. However, there is usually a price to pay, i.e. different sets of boundary conditions have to be imposed under different loading conditions, with the only exception of central reflection.

Properly formulated boundary conditions bring the effective strains at the upper length scale (they are in fact average strains at lower length scale) into the UC concerned. They have been referred to as the Kdofs, which are the crucial part of the UC concerned, and also offer a profound convenience to the process of material characterisation. Whilst the 'displacement' at each key dof gives the corresponding effective strain directly, the 'nodal force' at this dof is simply related to the effective stress or average stress in the UC. They do not only simplify the post-processing greatly, but can also be seen vividly as the link between the two length scales involved.

The significance of 'sanity checks' simply cannot be overstated. In fact, for any newly created UC, passing these checks is the most demanding task. The credibility of any UC not subjected to these checks should never be accepted. Failing any check signifies at least a mistake somewhere beyond any doubt. Resorting to experimental validations without these checks is deemed dodgy and futile.

The rules of formulating UCs can readily be applied to modern textile composites, both 2D and 3D. Their extension to other physical field, e.g. a wide range of physical processes classified under the diffusion problems, such as heat/electric conduction, fluid permeability in porous medium, etc. is straightforward. The RVEs and UCs as formulated in this chapter can be employed to characterise the relevant diffusion coefficients effectively.

The formulations of RVEs and UCs as presented in this chapter often appear to be tedious. However, they are systematic and hence suitable for programming. Readers are reminded that the finite element method was unthinkable to apply manually, but, once coded appropriately, it has become a universally applicable tool, without which modern engineering can hardly sustain itself. The claimed systematic nature has been demonstrated through a code, UnitCells©, as a secondary development of Abaqus/CAE [20, 21].

References

[1]   Nye, J.F., 1985. *Physical Properties of Crystals*. Clarendon Press, Oxford
[2]   Li, S. and Zou, C., 2011. The use of central reflection in the formulation of unit cells for micromechanical FEA, *Mech Mater,* **43**:824–834
[3]   Li, S. and Reid, S.R., 1992. On the symmetry conditions for laminated fibre-reinforced composite structures, *Int J Solids Struct.* **29**:2867-2880

[4] Li, S., 1999. On the unit cell for micromechanical analysis of fibre-reinforced composites, *Proc R Soc Lond A,* **455:**815-838

[5] Li, S., 2001. General unit cells for micromechanical analyses of unidirectional composites, *Composites A,* **32**:815-826

[6] Li, S. and Wongsto, A., 2004. Unit cells for micromechanical analyses of particle-reinforced composites*, Mech Mater,* **36:**543–572

[7] Li, S., Kyaw, S. and Jones, A., 2014. Boundary conditions resulting from cylindrical and longitudinal periodicities, *Comput Struct*, **133**:122-130

[8] Whitcomb, J., Chapman, C. D., and Tang, X., 2000. Derivation of boundary conditions for micromechanics analyses of plain and satin woven composites, *J Compos Mater*, **34**:724-747

[9] Washizu, K., 1982, *Variational Methods in Elasticity and Plasticity*, 3rd Edn., Pergamon Press, Oxford, England

[10] Li, S., 2008. Boundary conditions for unit cells from periodic microstructures and their implications, *Compos Sci Technol,* **68**: 1962–1974

[11] ASTM D3039/D3039M-14, Standard Test Method for Tensile Properties of Polymer Matrix Composite Materials

[12] BS EN ISO 527-4, Plastics. Determination of tensile properties. Test conditions for isotropic and orthotropic fibre-reinforced plastic composites, 1997

[13] Li, S. 2016. Symmetries in micro/meso-structures and their implications on material characterisation, unpublished work.

[14] Ahuja, N. and Schachter, B.J. 1983. *Pattern models*. Wiley, New York.

[15] Fang, Z., Yan, C., Sun, W., Shokoufandeh, A. and Regli, W., 2005. Homogenization of heterogeneous tissue scaffold: A comparison of mechanics, asymptotic homogenization, and finite element approach, *Applied Bionics and Biomechanics*. **2**(1):17-29

[16] Wongsto, A. and Li, S. 2005. Micromechanical FE analysis of UD fibre-reinforced composites with fibres distributed at random over the transverse cross-section, *Composites A,* **36**:1246–1266

[17] Li, S., Singh, C. and Talreja, R. 2009. A representative volume element based on translational symmetries for FE analysis of cracked laminates with two arrays of cracks, *Int. J Solids Struct*, **46**: 1793-1804

[18] Suquet, P., 1987. Elements of homogenization for inelastic solid mechanics, in: Homogenization Techniques for Composite Media, Sanchez-Palencia, E. and Zaoui, A. (Eds), Lecture Notes in Physics 272, Springer-Verlag, Berlin, 194–278

[19] S. Li, N. Warrior, Z. Zou and F. Almaskari, A unit cell for FE analysis of materials with the microstructure of a staggered pattern, *Composites A*, 42:801–811, 2011

[20] Li, S., Jeanmeure, L.F.C. and Pan, Q. 2015. A composite materials characterisation tool— UnitCells, *J Eng Math*, **95**:279–293

[21] Li, S. 2014. UnitCells© User Manual, Version 1.4

[22] Li, S., 2012. On the nature of periodic traction boundary conditions in micromechanical FE analyses of unit cells, *IMA J Appl Math*, **77**:441–450

[23] Li, S., Zhou, C., Yu, H., Li, L., 2011. Formulation of a unit cell of a reduced size for plain weave textile composites, *Comp Mater Sci*, **50**:1770-178

[24] Qian, C., Harper, L.T., Turner, T.A. Li, S. and Warrior, N.A., 2012. Determination of the size of representative volume elements for discontinuous fibre composites, *Comp Mater Sci*, **64**:106-111

[25] Qian, C., Harper, L.T., Turner, T.A. Li, S. and Warrior, N.A., 2012. Representative Volume Elements for Discontinuous Carbon Fibre Composites. Part 1: Boundary Conditions, *Compos Sci Technol*, **72**:225-234

[26] Qian, C., Harper, L.T., Turner, T.A. Li, S. and Warrior, N.A., 2012. Representative Volume Elements for Discontinuous Carbon Fibre Composites. Part 2: Determining the critical size, *Compos Sci Technol,* **72**:204-210

[27] Chen, L., Tao, X.M., and Choy, C.L., 1999. On the microstructure of three-dimensional braided preforms, *Compos Sci Technol*, **59**:394-404

[28] Li, S., Zhou, C., Huang, D. and Pan, Q., 2012. Unit cells for 3d braided textile composites, unpublished paper

[29] Li, H., Li, S., Wang, Y., Kandare, E., Kandola, B.K., Myler, P. and Horrocks, A. R. 2011. Micromechanical finite element analyses of woven fabric composites at elevated temperatures using unit cells at multiple length scales, *Comp Mater Sci,* **55**:23–33

[30] Li, H., Li, S. and Wang, Y. 2011. Prediction of effective thermal conductivities of woven fabric composites using unit cells at multiple length scales, *J Mater Res,* **26**(3):384-394

[31] Gou, J.-J. , Zhang, H., Dai, Y.-J., Li, S. and Tao, W.-Q. 2015. Numerical prediction of effective thermal conductivities of 3d four-directional, braided composites, *Compos Struct*, **125**:499-508

[32] Gou, J.-J., Ren, X.-J., Dai, Y.-J., Li, S. and Tao, W.-Q. 2016. Study of thermal contact resistance of rough surfaces based on the practical topography, to appear in *Comput Fluids*, **http://dx.doi.org/10.1016/j.compfluid.2016.09.018**